

Random Planted Forest: A Directly Interpretable Tree Ensemble

Munir Hiabu

Department of Mathematical Sciences, University of Copenhagen
and

Enno Mammen*

Institute for Applied Mathematics, Heidelberg University
and

Joseph T. Meyer*

Institute for Applied Mathematics, Heidelberg University

December 22, 2024

Abstract

We introduce a novel interpretable, tree based algorithm for prediction in a regression setting in which each tree in a classical random forest is replaced by a family of planted trees that grow simultaneously. The motivation for our algorithm is to estimate the unknown regression function from a functional decomposition perspective, where each tree corresponds to a function within that decomposition. The maximal order of approximation in the decomposition can be specified or left unlimited. If a first order approximation is chosen, the result is an additive model. In the other extreme case, if the order of approximation is not limited, the resulting model places no restrictions on the form of the regression function. In a simulation study we find encouraging prediction and visualisation properties of our random planted forest method. We also develop theory for an idealised version of random planted forests in cases where the maximal order of approximation is low. We show that if the order is smaller than three, the idealised version achieves asymptotically optimal convergence rates up to a logarithmic factor. ¹

Keywords: Random Forest; Interpretable Machine Learning; Functional Decomposition; Backfitting.

*We gratefully acknowledge support by the Deutsche Forschungsgemeinschaft (DFG) through the Research Training Group RTG 1953.

¹Code is available on GitHub: <https://github.com/PlantedML/randomPlantedForest>.

1 Introduction

In many ways, machine learning has been very disruptive in the last two decades. The class of neural networks has shown unprecedented and previously unthinkable predictive accuracy in fields such as image recognition (Rawat and Wang, 2017; LeCun et al., 2015), speech recognition (Hinton et al., 2012), and natural language processing (Collobert et al., 2011). Deep neural networks are strong in applications where huge amounts of data can be assembled and many variables interact with each other. A second disruptive class of machine learning algorithms are decision tree ensembles. The gradient boosting machine (Friedman, 2001) in particular excels in many applications. It often is the best performing algorithm for tabular data (Grinsztajn et al., 2022) and as such it is praised by many practitioners. Among the 29 challenge-winning solutions posted on Kaggle during 2015, 17 used xgboost – a variant of a gradient boosting machine (Chen and Guestrin, 2016). The second most popular method, deep neural networks, was used in 11 solutions.

These two classes of machine learning algorithms are in contrast to classical statistical models that assume an explicit structure such as a linear model (Nelder and Wedderburn, 1972) or an additive model (Friedman and Stuetzle, 1981; Buja et al., 1989). Traditionally, if the data does not fit into the required structure, the analyst tries to transform the variables at hand to achieve better fits – for example by using a log-transformation. Estimators received from the classical statistical models are highly accurate if the model is correctly specified. However, they perform poorly if the data deviates strongly from the structure assumed by the model.²

Our aim is to combine the best of the two worlds. We propose a new tree based algorithm we

²There are also fully nonparametric estimators which do not assume a specific structure, e.g., local polynomial estimators. However these are exposed to the curse of dimensionality, i.e. exponentially deteriorating estimation performance with growing number of variables.

call random planted forests (rpf). It starts with a simple structure and becomes increasingly flexible in a data-driven way as the algorithm unfolds.

We believe that one important factor of the success of gradient boosting is that it indirectly limits the order of interaction between predictors by limiting the depth of the trees. Thus, higher order interaction terms are ignored which usually require a large amount of data to be predicted accurately. This heuristic is also supported by Tan et al. (2022) who find that random forests perform poorly in additive models and by their proposal to look for modifications of random forests that adapt to structures in the data. Motivated by this paper, in Tan et al. (2022) a modification of random forest was proposed where in each iteration the tree is replaced by a finite fixed number of trees that grow in parallel. We consider a regression problem and assume that the regression function can be well approximated by lower order terms in a functional decomposition

$$m(x) = \sum_{t \subseteq \{1, \dots, d\}} m_t(x_t) = m_\emptyset + \sum_{t \in \{1, \dots, d\}} m_{\{t\}}(x_t) + \sum_{t_1 < t_2} m_{\{t_1, t_2\}}(x_{t_1}, x_{t_2}) + \dots \quad (1)$$

The rpf algorithm approximates this decomposition by hierarchically estimating the summands from lower to higher order interaction terms. Figure 1 provides a short illustration. The interaction terms included can be selected in advance. For example, one can fix the maximum order of approximation in the decomposition. If all interaction terms of all orders are included one has the full model where no restrictions are applied to the regression function. Uniqueness of the components is ensured via identification constraints, see supplement Section A.2. In contrast to the problem considered by Apley and Zhu (2020), the constraint itself is of secondary importance. The reason is that we do not aim to approximate a multivariate estimator by (1). The rpf estimator is already in the form of (1). Hence, the constraint does not have an effect on the quality of the estimator.

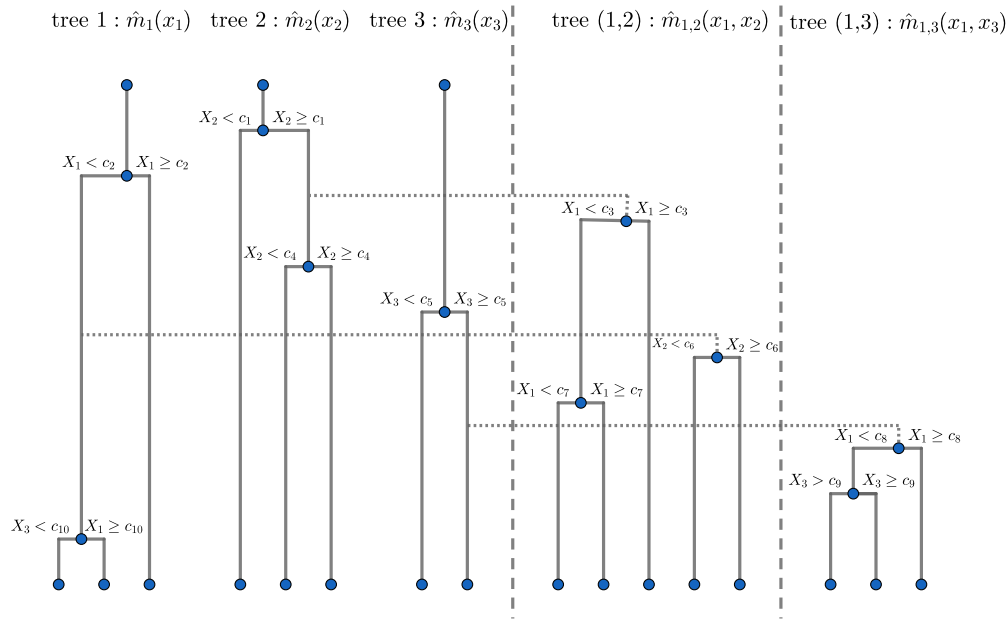


Figure 1: Illustration of a family of planted trees. Higher order trees are descendants of lower order trees. Trees grow simultaneously and the height of the edges indicate the order in which splits occur.

In the simulation study presented in Section 4, we find that even if the order of approximation in the rpf algorithm is not bounded the results are promising. However, bounding the order of interaction does increase the performance slightly if the true model satisfies the same constraint. An additional advantage of choosing a first or second order approximation is that the prediction can be visualised easily. Figure 2, Figure 3, and Figure 4 show plots that visualise additive and two dimensional components of a high dimensional model, respectively. The models we compare to were chosen since they are the strongest competitors which are easily visualisable regarding the simulation results in Section 4. Our rpf algorithm differs from classical random forests in several respects:

- Each tree in a random forest is replaced by a tree family. Each tree in a family corresponds to one term in the decomposition. The trees grow simultaneously and the global fit is given by the sum of the tree estimates.
- The algorithm for a tree family starts by growing main effect trees. Interaction

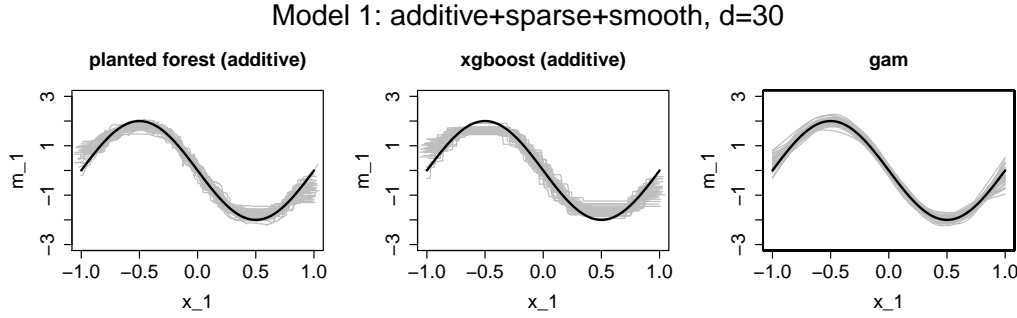


Figure 2: Estimates from 40 simulations for m_1 of Model 1: $m(x_1, \dots, x_{30}) = m_1(x_1) + m_2(x_2)$ with $m_k(x_k) = 2(-1)^k \sin(\pi x_k)$. The true function is visualised as a black solid line. Sample size is $n = 500$. Predictors have an approximate pairwise correlation of 0.3 and the noise has variance 1. For rpf and xgboost, parameters are picked from a grid search. The gam curves have data-driven parameters.

trees of order two are generated as descendants of main effect trees. More generally, interaction trees of higher order come from interaction trees of one degree less.

- As in classical random forests, splits are only allowed in a random subset of variables. This is done to reduce dependence between tree families with the aim of decreasing the variance of the forest estimator. Constructing random subsets is more involved in the rpf algorithm because different trees in one family have different dimensions. We call the parameter controlling the size of these random subsets `t_try`.
- Split points are selected from a finite set of random points. Not considering all possible points for splitting reduces computation time. Choosing random points further reduces the dependence between tree families. Additionally, bias is reduced in the case of smooth components. This can be deducted from our simulation study as well as theory developed in Section 5. We call the parameter controlling the number of possible split points `split_try`.

The idea of using splits from a finite set of random points is very similar to the method used in extremely random forests (Geurts et al., 2006).

Model 4: additive+sparse+jump, d=30

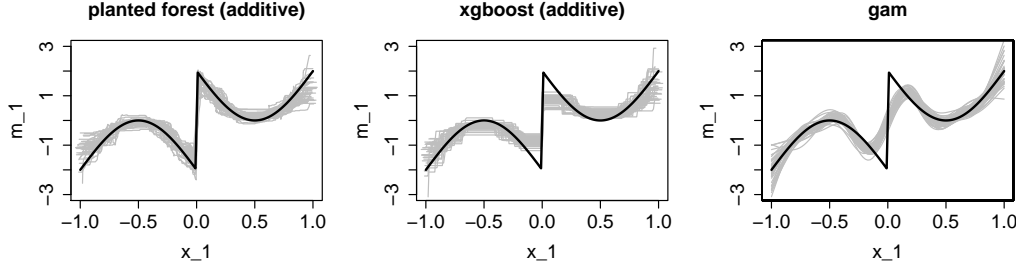


Figure 3: Estimates from 40 simulations for m_1 of Model 4: $m(x_1, \dots, x_{30}) = m_1(x_1) + m(x_2)$ with $m_k(x_k) = (2(-1)^k \sin(\pi x_k) - 2)\mathbb{1}(x \geq 0) + (-2 \sin(\pi x_k) + 2)\mathbb{1}(x < 0)$. The true function is visualised as a black solid line. Sample size is $n = 500$. Predictors have an approximate pairwise correlation of 0.3 and the noise has variance 1. For rpf and xgboost parameters are picked from a grid search. The gam curves have data-driven parameters.

Model 3: hierarchical-interaction+sparse+jump, d=30

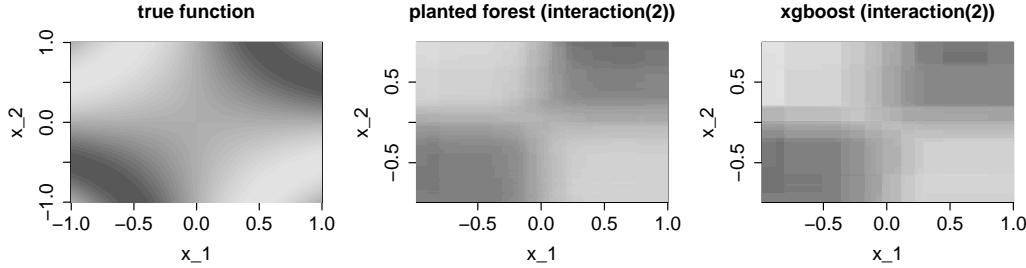


Figure 4: Heatmap from the median performing run for each method, measured via mean squared error, out of 40 simulations. Predictions are for $m_{1,2}$ of Model 3: $m(x_1, \dots, x_{30}) = \sum_{k=1}^3 m_k(x) + \sum_{1 \leq k < j \leq 3} m_{k,j}(x_k, x_j)$ with $m_{k,j}(x_k, x_j) = 2(-1)^k \sin(\pi x_k x_j)$, $m_k(x_k) = (-1)^k 2 \sin(\pi x_1)$. Sample size is $n = 500$. The predictors have an approximate pairwise correlation of 0.3 and the noise has variance 1. Parameters are picked from a grid search.

A tree family in the rpf algorithm can be thought of as one traditional decision tree in which a leaf is not removed from the algorithm when split in some cases. This happens when a leaf is split with respect to a component which was not used to construct the leaf so far. Additionally, each leaf may not be constructed by using more than r covariates. A simple heuristic why it may be beneficial not to remove a leaf from a tree when splitting is the following. Consider the regression problem $Y_i = m(X_i) + \epsilon_i$ with $i = 1, \dots, n$ and $m(x) = \sum_{j=1}^d \mathbb{1}(x_j \leq 0.5)$ for large d . If we never remove the original leaf, one can approximate m by splitting the original leaf once with respect to each covariate j . Thus, for each

direction, n data points are considered for finding the optimal split value. Additionally we end up with on average $n/2$ data points in each leaf. In the original random forests algorithm, in order to find a similar function, one would have to grow a tree with depth d , where each leaf is constructed by splitting once with respect to each covariate. This implies that we end up with 2^d leaves, which on average contain $n/(2^d)$ data points. Thus, the estimation should be much worse both because of less precise split points and less accurate fitted values.

If we only allow for a maximum interaction of two or less, the rpf algorithm provides an estimator which is easily interpretable. In recent years, there have been other algorithms with similar benefits: The rpf method differs from the tree based explainable boosting machine (Lou et al., 2012, 2013; Caruana et al., 2015; Lengerich et al., 2020) and the neural network based neural additive model (Agarwal et al., 2020) recently introduced in several ways. Similar to rpf, these methods aim to approximate the regression function via the functional decomposition (1). However, they rather resemble classical statistical methods described earlier. After specifying a fixed structure, the explainable boosting machine assumes that every component is relevant and all components are fitted via a backfitting algorithm (Breiman and Friedman, 1985). A similar principle using backpropagation instead of backfitting is applied in the neural additive model. In contrast, the rpf algorithm may ignore certain components completely. Additionally, interaction terms do not need to be specified beforehand. Hence explainable boosting machine and the neural additive model do not share two key strengths that rpf has: a) automatic interaction detection up to the selected order, b) strong performance in sparse settings.

Some model-based boosting algorithms (Hofner et al., 2014) have similar properties to the ones given above. In particular, they also suffer from the fact that they do not have au-

tomatic interaction detection, especially if a large number of covariates are present. An algorithm not suffering from this problem is multivariate adaptive regression splines (Friedman, 1991). However, it has a continuous output as composition of hinge functions. Thus, it does not adapt well when single jumps are present. Furthermore, as seen in our simulation study in Section 4, multivariate adaptive regression splines are less accurate when many covariates are active. A related algorithm which copes well with interaction terms is bayesian additive regression trees (Chipman et al., 2010). As seen in our simulation study in Section 4, the algorithm is competitive in all cases considered. However, bayesian additive random trees provides an estimator which does not follow a functional decomposition. Thus, it does not allow for interpretability as rpf does. Additionally, the MCMC method required is computationally expensive.

In Section 5, we develop theory for an idealised version of rpf. From a theoretical point of view, the most comparable algorithm to rpf is random forests. A theoretical study of Breiman’s original version of random forests (Breiman, 2001) is rather complex due to the double use of data, once in a CART splitting criterion and once in the final fits. Scornet et al. (2015) provide a consistency proof for Breiman’s algorithm while assuming an underlying additive model. They also show that the forest adapts to sparsity patterns. In more recent papers, theory has been developed for subsampled random forests. By linking to theory of infinite order U-statistics, asymptotic unbiasedness and asymptotic normality has been established for these modifications of random forests, see Mentch and Hooker (2016, 2017), Wager and Athey (2018), Peng et al. (2019). In our analysis of rpf, we assume that the splitting values do not depend on the response variable. In this respect, we follow a strand of literature on random forests, see e.g. Biau (2012) and Biau et al. (2008). Thus, we circumvent theoretical problems caused by the double use of data as in Breiman’s random

forest. We leave it to future research to study the extent to which theory introduced here carries over to random forests with data-dependent splitting rules, in particular for the case of random forests based on subsampling or sample-splitting. For a review of theoretical aspects of random forests, we also refer to Biau and Scornet (2016).

The paper is structured as follows. In Section 2, we introduce and explain the rpf algorithm in detail. In Section 3, the influence of various parameters is discussed. Additionally, we explain the intuition behind choices made in the construction of the algorithm. In Section 4, we perform a simulation study and compare our rpf algorithm to various other methods. Section 5 is a theoretical section. Among others, we show that an algorithm related to the rpf algorithm achieves asymptotically optimal convergence rates up to a logarithmic factor when the maximum order of approximation $r \leq 2$.

2 Random Planted Forests

In the following, we describe the rpf algorithm. We are handed data $(Y_i, X_{i,1}, \dots, X_{i,d})_{i=1}^n$ consisting of i.i.d. observations with $Y_i, X_{i,k} \in \mathbb{R}$. We consider the regression problem

$$E[Y_i | X_i = x] = m(x),$$

with the goal of estimating m . We assume that m can be approximated well by a functional decomposition (Stone, 1994; Hooker, 2007; Chastaing et al., 2012)

$$m(x) = \sum_{t \in T_r} m_t(x_t), \tag{2}$$

with a specified maximum order of approximation $r = 1, \dots, d$, where

$$T_r := \{t \subset \{1, \dots, d\} \mid |t| \leq r\}.$$

Note that m_\emptyset is a constant. Rpf is based on tree-like structures, which we refer to as trees for simplicity. A tree consists of a set of dimensions $t \in T_r$, a finite class of subsets $\{\mathcal{I}_{t,1}, \dots, \mathcal{I}_{t,p}\}$ and values $m_{t,1}, \dots, m_{t,p} \in \mathbb{R}$. For $t \in T_r$ and $i = 1, \dots, p$, the sets $\mathcal{I}_{t,i}$, which we refer to as leaves, are hyperrectangles

$$\mathcal{I}_{t,i} \in \left\{ \prod_{j=1}^d A_j \mid A_j \in \mathcal{A} \text{ for } j \in t, A_j = \mathbb{R} \text{ for } j \notin t \right\} \quad (3)$$

with

$$\mathcal{A} = \{A \subseteq \mathbb{R} \mid A = (b, c] \text{ or } A = (b, \infty) \text{ for } b \in [-\infty, \infty), c \in \mathbb{R}\}.$$

The corresponding estimator for m_t is given by

$$\hat{m}_t(x) = \sum_{j=1}^p m_{t,j} \mathbb{1}(x \in \mathcal{I}_{t,j}).$$

Note that for any $x \in \mathbb{R}^d$, due to (3), \hat{m}_t only depends on the value of x_t . The sets $\mathcal{I}_{t,j}$ are obtained by an iterative procedure, where in each step a leaf is selected and split into two new leaves. In the following, we usually call the components m_t trees. In the definition of trees in the literature, the leaves of a tree typically form a partition of the domain. However, in general, the leaves of trees in the rpf algorithm are neither disjoint, nor do they unify to the domain. The algorithm provides an estimator of the regression function m from an ensemble of tree families. Each tree family estimates the function m from a bootstrap sample. The final estimator is the average of the estimators derived from the

different tree families. A family of planted trees consists of a tree for each set of coordinates $t \in T_r$, where a tree is grown using only information on its respective coordinates. Thus, the resulting estimator is in the form of (2).

An illustration of the algorithm unfolding for a family of planted trees is given in Figure 1. Nodes correspond to leaves. The children of a leaf are connected via edges and are located below the respective node. The vertical position of a node indicates when the split occurred. The final leaves are located at the bottom. If a node is connected to a node above via a dashed edge, this represents a split where the original leaf is not replaced. This happens when growing from one tree to another. The example given here includes three coordinates. Each data point is contained in between three and six leaves.

We proceed by explaining the algorithm precisely, including most technical details. We start by introducing the calculation of a split in Subsection 2.1 followed by the iterations in Subsection 2.2. We conclude with the extension to a forest and a discussion on the driving parameters.

2.1 Calculating a Split

We are handed a coordinate $k \in \{1, \dots, d\}$, a tree $t \in T_r$, a set $\mathcal{I} \subseteq \mathbb{R}^d$, a current value $m_{\mathcal{I}}$, residuals R_i , observations X_i , and a value $c \in \mathbb{R}$. Define a partition $\mathcal{I} = \mathcal{I}^+ \cup \mathcal{I}^-$ by

$$\mathcal{I}^+ := \{x \in \mathcal{I} \mid x_k > c\}, \quad \mathcal{I}^- := \{x \in \mathcal{I} \mid x_k \leq c\}.$$

Let $g_{\mathcal{I}^+} := \sum_{X_i \in \mathcal{I}^+} R_i / \sum_{X_i \in \mathcal{I}^+} 1$, $g_{\mathcal{I}^-} := \sum_{X_i \in \mathcal{I}^-} R_i / \sum_{X_i \in \mathcal{I}^-} 1$ and

$$g_{\mathcal{I},c} : \mathbb{R}^d \rightarrow \mathbb{R}, \quad g_{\mathcal{I},c}(x) = \mathbb{1}(x \in \mathcal{I}^+)g_{\mathcal{I}^+} + \mathbb{1}(x \in \mathcal{I}^-)g_{\mathcal{I}^-}.$$

Note that $g_{\mathcal{I},c}$ is constant on each of the sets \mathcal{I}^+ , \mathcal{I}^- and $\mathbb{R}^d \setminus \mathcal{I}$. Using the function $g_{\mathcal{I},c}$, we update the residuals $R_i^{\text{new}} := R_i - g_{\mathcal{I},c}(X_i)$ and values

$$m_{\mathcal{I}^+}^{\text{new}} := m_{\mathcal{I}} + g_{\mathcal{I}^+}, \quad m_{\mathcal{I}^-}^{\text{new}} := m_{\mathcal{I}} + g_{\mathcal{I}^-}.$$

Pseudo-code of this procedure is given in Algorithm 1.

Algorithm 1 Calculating a Split

Input $k, t, \mathcal{I}, c, m_{\mathcal{I}}, R_1, \dots, R_n, X_1, \dots, X_n$
Calculate $\mathcal{I}^+, \mathcal{I}^-$
for $i = 1, \dots, n$ **do**
 $R_i := R_i - g_{\mathcal{I},c}(X_i);$
Calculate $m_{\mathcal{I}^+} := m_{\mathcal{I}} + g_{\mathcal{I}^+}; \quad m_{\mathcal{I}^-} := m_{\mathcal{I}} + g_{\mathcal{I}^-}$
Output $m_{\mathcal{I}^+}, m_{\mathcal{I}^-}, \mathcal{I}^+, \mathcal{I}^-, R_1, \dots, R_n$

2.2 Planted tree family

We start off by setting the residuals $R_i^{(0)} := Y_i$ for $i = 1, \dots, n$. We set a single leaf $\mathcal{I}_{\emptyset,1}^{(0)} := \mathbb{R}^d$ and thus the number of leaves for $t = \emptyset$ is $p_{\emptyset}^{(0)} = 1$. The corresponding value is $m_{\emptyset,1} = 0$. The trees $t \neq \emptyset$ have no starting leaves and thus, $p_t^{(0)} = 0$.

An iteration step is carried out as follows. In step s we are handed residuals $R_i^{(s-1)}$, leaves $\mathcal{I}_{t,1}^{(s-1)}, \dots, \mathcal{I}_{t,p_k^{(s-1)}}^{(s-1)}$ and values $m_{t,1}^{(s-1)}, \dots, m_{t,p_k^{(s-1)}}^{(s-1)}$. The leaves are of the form (3). In each step s , we select a tree t_s , a coordinate $k_s = 1, \dots, d$, an index $j_s = 1, \dots, p_{t_s}^{(s-1)}$, and a split point c_s in order to split $\mathcal{I}_{t_s,j_s}^{(s-1)}$ using Algorithm 1. The chosen combination must be viable in the sense that it must fulfill the following three conditions.

$$(C_1) \quad p_{t_s}^{(s-1)} \geq 1.$$

$$(C_2) \quad \text{If } |t_s| = r, \text{ then } k_s \in t_s.$$

(C₃) We have

$$\{i \in \{1, \dots, n\} \mid X_{i,k_s} \in \mathcal{I}, X_{i,k_s} > c_s\}, \{i \in \{1, \dots, n\} \mid X_{i,k_s} \in \mathcal{I}, X_{i,k_s} \leq c_s\} \neq \emptyset.$$

Algorithm 2 Random Planted Trees

Input $(Y_1, X_1), \dots, (Y_n, X_n)$
 $R_i \leftarrow Y_i; \quad \mathcal{I}_{\emptyset,1} \leftarrow \mathbb{R}^d; \quad m_{\emptyset,1} \leftarrow 0; \quad p_t \leftarrow 0; \quad p_{\emptyset} \leftarrow 1$
for $s = 1, \dots, \text{nsplits}$ **do**
 Calculate t_s, k_s, j_s, c_s using Equation (4)
 $k \leftarrow k_s; \quad t \leftarrow t_s; \quad \mathcal{I} \leftarrow \mathcal{I}_{t_s, j_s};$
 if $k_s \in t_s$ **then**
 $m_{\mathcal{I}} \leftarrow m_{t_s, j_s}$
 Calculate $m_{\mathcal{I}^+}, m_{\mathcal{I}^-}, \mathcal{I}^+, \mathcal{I}^-, R_1, \dots, R_n$ (Algorithm 1)
 $\mathcal{I}_{t_s, j_s} \leftarrow \mathcal{I}^+; \quad \mathcal{I}_{t_s, p_{t_s}+1} \leftarrow \mathcal{I}^-$
 $m_{t_s, j_s} \leftarrow m_{\mathcal{I}^+}; \quad m_{t_s, p_{t_s}+1} \leftarrow m_{\mathcal{I}^-}; \quad p_{t_s} \leftarrow p_{t_s} + 1$
 else
 $m_{\mathcal{I}} \leftarrow 0$
 Calculate $m_{\mathcal{I}^+}, m_{\mathcal{I}^-}, \mathcal{I}^+, \mathcal{I}^-, R_1, \dots, R_n$ (Algorithm 1)
 $t_s \leftarrow t_s \cup k_s$
 $\mathcal{I}_{t_s, p_{t_s}+1} \leftarrow \mathcal{I}^+; \quad \mathcal{I}_{t_s, p_{t_s}+2} \leftarrow \mathcal{I}^-$
 $m_{t_s, p_{t_s}+1} \leftarrow m_{\mathcal{I}^+}; \quad m_{t_s, p_{t_s}+2} \leftarrow m_{\mathcal{I}^-}; \quad p_{t_s} \leftarrow p_{t_s} + 2$

Now, there are two cases with different updating procedures for the corresponding estimators. If $k_s \in t_s$, we use $m_{\mathcal{I}} := m_{t_s, j_s}^{(s-1)}$ as an input for Algorithm 1. The leaf $\mathcal{I}_{t_s, j_s}^{(s-1)}$ is replaced by \mathcal{I}^+ and \mathcal{I}^- in tree t_s . If $k_s \notin t_s$, we use $m_{\mathcal{I}} := 0$ as an input for Algorithm 1. The sets $\mathcal{I}^+, \mathcal{I}^-$ are added to the tree $\{k_s\} \cup t_s$. The corresponding values and residuals are updated according to Algorithm 1. In order to select t_s, k_s, j_s , and c_s , we use the CART methodology. For suitable t, k, j , and c , let $R_i^{t,k,j,c}$ denote the residual one obtains by using Algorithm 1 with inputs $k, t, \mathcal{I} := \mathcal{I}^{(s-1)}(t, j), c$, and $m_{\mathcal{I}} := m_{t,j}^{(s-1)}$, if $k \in t, m_{\mathcal{I}} := 0$ otherwise. We now select t_s, k_s, j_s , and c_s as

$$(t_s, k_s, j_s, c_s) := \arg \min_{t,k,j,c} \sum_{i=1}^n (R_i^{t,k,j,c})^2. \quad (4)$$

Note that this procedure guarantees that the leaves $\mathcal{I}_{t,j}^{(s)}$ of every tree t_s are of the form (3) for all s . Therefore, they are easy to keep track of. The algorithm stops after **nsplits** iterations. Pseudo-code of this procedure is given in Algorithm 2.

2.3 From a tree family to a Forest

In order to reduce variance, an extension of Algorithm 2 similar to the random forest procedure is considered. We draw **ntrees** independent bootstrap samples $(Y_1^b, X_1^b), \dots, (Y_n^b, X_n^b)$ from our original data. On each of these bootstrap samples, we apply Algorithm 2 with two minor adjustments. Instead of minimizing over all $c \in \mathbb{R}$ satisfying the constraint (C_3) , in each iteration we uniformly at random select **split_try** values for each coordinate in each leaf \mathcal{I} in each tree t . For each coordinate k , the values are chosen (with replacement) from

$$\{X_{i,k} \mid X_{i,k} \in \mathcal{I}, X_{i,k} \neq \max\{X_{i,j} \mid X_{i,j} \in \mathcal{I}\}\}.$$

Secondly, define a set representing the viable combinations

$$V_r := \{(k, t) \in \{1, \dots, d\} \times T_r \mid k \in t, \max\{p_t, p_{t \setminus k}\} \geq 1\}$$

In each iteration step we select a subset $M \subseteq V_r$ uniformly at random, where $|M| = \lceil |V_r| \cdot \mathbf{t_try} \rceil$ for some given value $\mathbf{t_try} \in (0, 1]$. In step 4, when calculating (t_s, k_s, j_s, c_s) in Equation (4), we minimize under the additional conditions that c is one of the **split_try** values and $(k_s, t_s) \in M$ or $(k_s, t_s \setminus k_s) \in M$. The resulting estimators are $\hat{m}_t^b(x) := \sum_{j=1}^{p_t^b} \mathbb{1}(x \in \mathcal{I}_{t,j}^b) m_{t,j}^b$ for $b = 1, \dots, \mathbf{ntrees}$. The overall estimators are given by

$$\hat{m}_t(x) := \frac{1}{\mathbf{ntrees}} \sum_{b=1}^{\mathbf{ntrees}} \hat{m}_t^b(x).$$

3 Discussion of Parameters

In this section, we shortly discuss the parameters introduced and explain why choices were made when designing the algorithm. Further remarks on the algorithm can be found in Section A in the supplement material.

3.1 `t_try`

In the rpf algorithm, the number of combinations of trees and coordinates considered in each iteration step is defined as a fixed proportion `t_try` of the number of viable combinations $|V|$. Thus, the number of combinations considered increases as the algorithm unfolds. We assessed many different similar mechanisms in order to restrict the number of combinations used in an iteration step. First of all, we found that using a random subset of the viable combinations instead of simply restricting the coordinates for splitting is far superior. Roughly speaking, the reason is that the algorithm may lock itself in a tree if all trees are splitable in each step. The question remains how to quantify the amount of combinations used. Selecting a constant number of viable combinations has the disadvantage of either allowing all combinations in the beginning or having essentially random splits towards the end of the algorithm. Thus, the number of combinations considered must depend on the number of viable combinations. While other functional connections between the number of viable and the number of considered combinations are possible, choosing a proportional connection seems natural.

3.2 `split_try`

In contrast to `t_try`, the parameter `split_try` implies an almost constant number of considered split points in each iteration. The `split_try` split options are selected uniformly

at random with replacement. In Section 4, we find that the optimal value for `split_try` is usually small compared to the data size. In our experience, setting a constant proportion either leads to totally random splits for small leaves or essentially allows all splits for large leaves. The reason is that for large leaves, if a small number of data points are added or removed, the estimation is basically the same. For the same reason, having a low amount of potential split points in a large leaf is not a problem. The version we use here yielded the best results. The choice `t_try` < 1 as well as only using `split_try` split points is done in order to reduce the correlation between tree families and additionally reducing bias in latter case. It also reduces computational cost. While it is not obvious which of the two parameters, `split_try` or `t_try`, should be lowered in order to reduce variance, our results significantly improved as soon as we introduced the mechanisms regarding the parameters.

3.3 Driving Parameters

Although the presence of the mechanisms involving `split_try` and `t_try` improve the results of `rpf`, the exact value they take on is not as relevant. Rather, we consider them to be fine-tuning parameters. Similarly, the number of tree families `ntrees` in a forest does not have much impact as long as `ntrees` is large enough; in our simulation study, `ntrees` = 50 seemed satisfactory. The main driving parameter for the estimation quality of `rpf` is the number of iteration steps `nsplits`. While the estimation is quite stable under small changes of `nsplits`, strongly lowering `nsplits` results in a bias, while vastly increasing the parameter leads overfitting.

4 Simulations

In this section, we conduct an extensive simulation study in order to arrive at an understanding of how the rpf algorithm copes with different settings and how it compares to other methods. For each of 100 Monte-Carlo simulations $s = 1, \dots, 100$, We consider the regression setup

$$Y_i^s = m(X_i^s) + \varepsilon_i^s, \quad i = 1, \dots, 500,$$

where $\varepsilon_i^s \sim N(0, 1)$ i.i.d. with twelve different models, i.e. different functional shapes of m . The models are outlined in Table 1. In sparse models, we consider cases with $d = 4, 10, 30$ predictors. For dense models we use $d = 4, 10$. Following Nielsen and Sperlich (2005), the predictors $(X_{i,1}^s, \dots, X_{i,d}^s)$ are distributed as follows. We first generate $(\tilde{X}_{i,1}^s, \dots, \tilde{X}_{i,d}^s)$ from a d -dimensional standard multi-normal distribution with mean equal to 0 and $\text{Cov}(\tilde{X}_{i,j}^s, \tilde{X}_{i,l}^s) = \text{Corr}(\tilde{X}_{i,j}^s, \tilde{X}_{i,l}^s) = 0.3$ for $j \neq l$. Then, we set

$$X_{i,k}^s = 2.5\pi^{-1}\arctan(\tilde{X}_{i,k}^s).$$

This procedure is repeated independently 500 times. The methods we compare are given in Table 2. Performance is evaluated by the average mean squared error (MSE) from 100 simulations. The MSE is evaluated on test points $X_{501}^s, \dots, X_{1000}^s$ which are generated independently of the data:

$$\frac{1}{100} \sum_{s=1}^{100} \frac{1}{500} \sum_{i=501}^{1000} \{m(X_i^s) - \hat{m}^s(X_i^s)\}^2,$$

where s runs over the different simulations and \hat{m}^s represents the estimator depending on the parameters in question as well as the data $(X_i^s, Y_i^s)_{i=1}^{500}$.

Table 1: Dictionary for model descriptions. In total we consider 12 models. Each model has a model structure (first six rows) as well as a function shape (last two rows). The constant d denotes the total number of predictors.

Description	Meaning
additive+sparse	$m(x) = m_1(x_1) + m_2(x_2)$
hierarchical-interaction	$m(x) = m_1(x_1) + m_2(x_2) + m_3(x_3)$
+sparse	$+m_{1,2}(x_1, x_2) + m_{2,3}(x_2, x_3)$
pure-interaction+sparse	$m(x) = m_{1,2}(x_1, x_2) + m_{2,3}(x_2, x_3)$
additive+dense	$m(x) = m_1(x_1) + \dots + m_d(x_d)$
hierarchical-interaction+dense	$m(x) = \sum_{k=1}^d m_k(x_k) + \sum_{k=1}^{d-1} m_{k,k+1}(x_k, x_{k+1})$
pure-interaction+dense	$m(x) = \sum_{k=1}^{d-1} m_{k,k+1}(x_k, x_{k+1})$
smooth	$m_k(x_k) = (-1)^k 2 \sin(\pi x_k)$ $m_{k,k+1}(x_k, x_{k+1}) = m_k(x_k x_{k+1})$
jump	$m_k(x_k) = \begin{cases} (-1)^k 2 \sin(\pi x_k) - 2 & \text{for } x \geq 0, \\ (-1)^k 2 \sin(\pi x_k) + 2 & \text{for } x < 0 \end{cases}$ $m_{k,k+1}(x_k, x_{k+1}) = m_k(x_k x_{k+1})$

Table 2: Dictionary for algorithms. In total we consider 7 different. Additionally, 2 toy algorithms are considered for benchmark values.

Description	short	Code-Reference
A gradient boosting variant	xgboost	Chen et al. (2020)
rpf	rpf	Supplement
Random forest	rf	Wright and Ziegler (2015)
Smooth backfitting ³	sbfb	Supplement
Generalized additive models ⁴	gam	Wood (2011)
Bayesian additive regression trees	BART	Sparapani et al. (2021)
multivariate additive regression splines	MARS	Hastie (2020)
1 nearest neighbours	1-NN	
Sample average	mean	

For xgboost and rpf, we record results for the case when the estimators are additive. Additionally, we show results for estimators which can approximate higher order interaction terms. For the rpf algorithm, we further distinguish between an estimator able to approximate interaction terms of order up to two as well as an unbounded configuration. Details are presented in Table 5 in the supplement. Beforehand, we ran 30 simulations to find the optimal parameter combinations for each method from the parameter options outlined in Table 5. These simulations were conducted independently from the final simulations

using training data $(\bar{X}_1^s, \bar{Y}_1^s), \dots, (\bar{X}_{500}^s, \bar{Y}_{500}^s)$ for $s = 1, \dots, 30$. A parameter combination was considered optimal if it minimized the mean squared error averaged over all 30 simulations. For xgboost and rpf, we also considered data-driven parameter choices (indicated by CV). We ran a 10-fold cross validation considering all parameters outlined in Table 5 including all sub-methods and options. The initial parameter options are hand-picked from preliminary simulation runs. Note that we did not optimize parameters for the method gam. Instead, we used a fully data-driven version. We now present the results from 100 Monte Carlo simulations. We only show selected parts of the overall study in the main part of this paper. Additional tables can be found in Section C in the supplement material.

Table 3: Model 1: Additive Sparse Smooth Model. We report the average MSE from 100 simulations. The standard deviations are provided in brackets.

Method	dim=4	dim=10	dim=30
xgboost (depth=1)	0.119 (0.021)	0.142 (0.021)	0.176 (0.027)
xgboost	0.141 (0.024)	0.166 (0.028)	0.193 (0.033)
xgboost-CV	0.139 (0.028)	0.152 (0.029)	0.194 (0.035)
rpf (max_interaction=1)	0.087 (0.018)	0.086 (0.017)	0.097 (0.019)
rpf (max_interaction=2)	0.107 (0.015)	0.121 (0.025)	0.142 (0.026)
rpf	0.112 (0.017)	0.134 (0.026)	0.162 (0.028)
rpf-CV	0.103 (0.02)	0.102 (0.035)	0.105 (0.022)
rf	0.209 (0.021)	0.252 (0.027)	0.3 (0.029)
sbfb	0.071 (0.026)	0.134 (0.013)	0.388 (0.073)
gam	0.033 (0.012)	0.035 (0.013)	0.058 (0.021)
BART	0.085 (0.019)	0.076 (0.017)	0.091 (0.023)
BART-CV	0.09 (0.019)	0.081 (0.014)	0.09 (0.02)
MARS	0.054 (0.014)	0.061 (0.025)	0.076 (0.031)
1-NN	1.509 (0.1)	3.228 (0.182)	5.534 (0.313)
average	3.811 (0.217)	3.689 (0.183)	3.748 (0.202)

Table 3 contains the additive sparse smooth setting. We observe that algorithms relying on continuous estimators (sbfb, gam, MARS) outperform the others with gam being the clear winner, irrespective of the number of predictors d . From the other algorithms, bayesian additive random trees and additive (**max_interaction=1**) rpf do best with similar performance between the two algorithms. Note that smooth backfitting (sbfb) falls off

considerably for $d = 10, 30$, hinting that it cannot take advantage of the sparsity condition. This is not surprising given that no penalty terms are used for the L_2 losses. Interestingly, random rpf (`max_interaction=2`) and rpf perform very well and even outperform the additive (`depth=1`) xgboost. Random forest (rf) shows the worst performance in this setting. However, it seems to catch up to smooth backfitting with increasing dimension, indicating that it makes better use of the sparsity condition.

In the hierarchical-interaction sparse smooth setting, which is visualized in Table 4, we only show results from methods which can deal with interactions. Other cases are deferred to the supplement material. Here, we find that BART as well as multivariate additive regression splines (MARS) outperform our rpf algorithm. However, the latter slightly outperforms xgboost. In the Table 10 in the supplement, a similar picture can be observed in the pure-interaction case. In particular, BART proves to be much stronger than all competing algorithms. This indicates that BART does not rely on a hierarchical interaction structure as much as the other methods. However, it comes at the cost of increased computational time. Recall that in contrast to rpf, MARS provides a continuous estimator and the estimator provided by BART is not interpretable. Next, we re-visit the additive case. However, this time, the regression function is not continuous. The results are tabulated in Table 6 in the supplement material. In this setting, our additive rpf algorithm and the BART algorithm perform best. A visual picture of the excellent fit of rpf was provided in Figure 3. Random forest and xgboost share the third position. The best interpretable competitor is xgboost (additive). Unsurprisingly, models based on continuous estimators can not deal with the jumps in the regression functions. Cases including interaction terms and jumps in the regression function are deferred to the supplement material.

We now consider dense models. In the additive dense smooth model, see Table 7 in the

Table 4: Model 2&3: Hierarchical and Pure Interaction Sparse Smooth Model. We report the average MSE from 100 simulations. The standard deviations are provided in brackets.

Method		dim=4	dim=10	dim=30
Hierarchical- interaction	xgboost	0.374 (0.035)	0.481 (0.064)	0.557 (0.089)
	xgboost-CV	0.393 (0.051)	0.499 (0.058)	0.563 (0.089)
	rpf (<code>max_interaction=2</code>)	0.248 (0.038)	0.327 (0.045)	0.408 (0.07)
	rpf	0.263 (0.034)	0.357 (0.044)	0.452 (0.076)
	rpf-CV	0.277 (0.039)	0.366 (0.051)	0.463 (0.083)
	rf	0.432 (0.039)	0.575 (0.061)	0.671 (0.08)
	BART	0.214 (0.03)	0.223 (0.04)	0.252 (0.037)
	BART-CV	0.242 (0.043)	0.276 (0.053)	0.315 (0.047)
	MARS	0.355 (0.089)	0.282 (0.038)	0.414 (0.126)
	1-NN	2.068 (0.156)	5.988 (0.624)	11.059 (0.676)
	average	8.366 (0.43)	8.086 (0.246)	8.207 (0.496)

supplement material, the clear winners are sbf and gam, with gam having the best performance. This is not surprising, since these methods have more restrictive model assumptions than the others. Therefore, if the assumptions are met, one would expect the methods to do well. Additionally, gam typically has an advantage over sbf in our setting. This is because splines usually fit trigonometric curves well, while kernel smoothers would be better off with a variable bandwidth in this case, which we did not implement. Observe that MARS does not deal well with this situation, in particular in the case $d=10$. Our rpf method is in third place, tied with BART and slightly outperforming xgboost. This suggests that the rpf algorithm is especially strong in sparse settings. In dense settings, the advantage towards xgboost and BART shrinks. This observation is underpinned by the next scenario. As a final setting, we consider the hierarchical-interaction dense smooth model. The results are tabulated in Table 8 in the supplement. The results further strengthen our intuition that the current version of the rpf algorithm performs worse in dense settings. While it is by far the best performing algorithm with only four predictors, the performance deteriorates faster than that of other methods when adding predictors. In dimension 10, i.e, with ten predictors, xboost outperforms rpf whereas the reverse can be observed for $d=4$.

Concluding remarks on simulations results From the conducted simulation study, we find that BART showed the strongest performance while the rpf algorithm is the runner-up. Compared to BART, rpf has the advantage that results can be easily plotted and interpreted (if only lower-interactions are fitted). Additionally, the BART algorithm is computationally quite intensive and we indeed struggled to get BART running in the higher dimensional cases without error already in our study with a sample size of 500 (probably because of memory limitations). Xgboost showed very strong results in terms of accuracy while being very fast and resources effective. However, accuracy turns out to be slightly worse than rpf in low-interaction settings and it does not provide the possibility to visualize the fit.

5 Theoretical properties

In this section we derive asymptotic properties for a slightly modified rpf algorithm. The main difference is that in the tree family construction of the modified forest estimator, splitting does not depend directly on the responses $(Y_i : i = 1, \dots, n)$. With this modification we follow other studies of forest based algorithms to circumvent mathematical difficulties which arise if settings are analyzed where the same data is used to choose the split points as well as to calculate the fits in the leaves. Clearly, one can apply the results in this section to a similar modification of rpf making use of data splitting to separate splitting and fitting. Our results imply two findings. First, for $r \leq 2$ the estimator can achieve optimal rates up to logarithmic terms in the nonparametric model where the interaction terms m_t (for $|t| \leq 2$) allow for continuous second order derivatives. Secondly, for all choices of r one achieves faster rates of convergence for the forest estimator than for tree family estimators that are based on calculating only one single tree family. We will comment below why the

situation changes for $r \geq 3$ compared to $r \leq 2$. A major challenge in studying rpf lies in the fact that the estimator is only defined as the result of an iterative algorithm and not as the solution of an equation or of a minimizing problem. In particular, our setting differs from other studies of random forests where tree estimates are given by leaf averages of terminal nodes. In such settings the tree estimator only depends on the leaves of terminal nodes, but not on other structural elements of the tree, and in particular not on the way the tree was grown. Secondly, the definition of the estimator as a leaf average allows for simplifications in the mathematical analysis. We cannot make use of either of these advantages. The main point of our mathematical approach is to show that approximately, the tree family estimators and the forest estimators are given by a least squares problem defined by the leaves of at the end of the algorithm. We assume that the regression function fulfills $m(x) := m^0(x) = \sum_{t \in T_r} m_t^0(x_t)$ for some $r \in \mathbb{N}$. The data is generated as

$$Y_i = m^0(X_i) + \varepsilon_i = \sum_{t \in T_r} m_t^0(X_{i,t}) + \varepsilon_i,$$

where the additive components $m_t^0 : t \in T_r$ are smooth functions. In the model equation, the ε_i 's are mean zero error variables, and, for simplicity, the covariables $X_{i,k}$ are assumed to lie in $[0, 1]$; $i = 1, \dots, n$; $k = 1, \dots, d$.

We now describe the iteration steps of the tree family algorithm discussed in this section. As initialisation we set $\mathcal{I}_{t,1}^0 = [0, 1]^d$, $L_{t,0} = 1$ and $\widehat{m}_t^0 \equiv 0$ for $t \in T_r$. In iteration steps $s = 1, \dots, S$ partitions $\mathcal{I}_{t,l}^s = \prod_{k \in t} (a_{t,k,l}^s, b_{t,k,l}^s] \times \prod_{k \notin t} (0, 1]$ of $[0, 1]^d$ with $l = 1, \dots, L_{t,s}$ are updated by splitting one of the rectangles $\mathcal{I}_{t,l}^s$ for one $t \in T_r$, one $l \in \{1, \dots, L_{t,s}\}$ along one coordinate k . Here, in abuse of notation, we write $\prod_{k \in t} \cdot \times \prod_{k \notin t} \cdot$ for the set of tuples with coordinates ordered according to the value of k and not according to the appearance in the product subindices. We now describe step s where the rectangles $\mathcal{I}_{t,l}^{s-1}$ are

updated. At step s one chooses a $t_s \in T_r$, an $l_s \in \{1, \dots, L_{t_s, s-1}\}$, a $k_s \in t_s$ and a splitting value $b_{t_s, k_s, l_s}^s \in (a_{t_s, k_s, l_s}^{s-1}, b_{t_s, k_s, l_s}^{s-1})$. The values are chosen by some random procedure that satisfies the assumptions $(A_1), \dots, (A_8)$ below. Using these values one splits $(a_{t_s, k_s, l_s}^{s-1}, b_{t_s, k_s, l_s}^{s-1}]$ into $(a_{t_s, k_s, l_s}^s, b_{t_s, k_s, l_s}^s]$ and $(a_{t_s, k_s, L_{t_s, s}}^s, b_{t_s, k_s, L_{t_s, s}}^s]$, where $a_{t_s, k_s, l_s}^s = a_{t_s, k_s, l_s}^{s-1}$, $a_{t_s, k_s, L_{t_s, s}}^s = b_{t_s, k_s, l_s}^s$, $b_{t_s, k_s, L_{t_s, s}}^s = b_{t_s, k_s, l_s}^{s-1}$ and $L_{t_s, s} = L_{t_s, s-1} + 1$. For $(k, l) \neq (k_s, l_s)$ we set $(a_{t_s, k, l}^s, b_{t_s, k, l}^s] = (a_{t_s, k, l}^{s-1}, b_{t_s, k, l}^{s-1}]$. Then we update the rectangle $\mathcal{I}_{t_s, l}^s$ for $l = l_s$ and $l = L_{t_s, s}$ by defining $\mathcal{I}_{t_s, l}^s = \mathcal{I}_{t_s, l}^{\text{marg}, s} \times \prod_{k \notin t_s} (0, 1]$ with $\mathcal{I}_{t_s, l}^{\text{marg}, s} = \prod_{k \in t_s} (a_{t_s, k, l}^s, b_{t_s, k, l}^s]$. All other rectangles are taken over identically from the last step. Finally, for the chosen tree t_s , the values $\hat{m}_{t_s}^s$ are updated by averaging residuals over the intervals $\mathcal{I}_{t_s, l}^s$ for $l = 1, \dots, L_{t_s, s}$. For a subset \mathcal{I} of $[0, 1]^d$ we write $|\mathcal{I}|$ for the Lebesgue measure of the set. Note that for finite sets Q , we also use $|Q|$ for the number of Elements in Q . From context, it will always be clear which version is used. Additionally, we write $|\mathcal{I}|_n = |\{i : X_i \in \mathcal{I}\}|/n$ for the empirical measure of \mathcal{I} . Then, for $x_{t_s} \in \mathcal{I}_{t_s, l}^{\text{marg}, s}$ with $l \in \{1, \dots, L_{t_s, s}\}$ the estimator can be written as

$$\hat{m}_{t_s}^s(x_{t_s}) = \frac{1}{n|\mathcal{I}_{t_s, l}^s|_n} \sum_{i: X_i \in \mathcal{I}_{t_s, l}^s} \left(Y_i - \sum_{t \in T_r, t \neq t_s} \hat{m}_t^{s-1}(X_{i, t}) \right).$$

Because \hat{m}_t^{s-1} is constant on the set $\mathcal{I}_{t, k}^s$ we can rewrite the formula with $\hat{m}_t^{s-1}(\mathcal{I}_{t, k}^s)$ equal to $\hat{m}_t^{s-1}(u)$ for $u \in \mathcal{I}_{t, k}^s$ as follows

$$\hat{m}_{t_s}^s(x_{t_s}) = \hat{\hat{m}}_{t_s}^s(x_{t_s}) - \frac{1}{|\mathcal{I}_{t_s, l}^s|_n} \sum_{t \in T_r, t \neq t_s} \sum_{k=1}^{L_{t, s}} |\mathcal{I}_{t_s, l}^s \cap \mathcal{I}_{t, k}^s|_n \hat{m}_t^{s-1}(\mathcal{I}_{t, k}^s).$$

Here for $x_{t_s} \in \mathcal{I}_{t_s, l}^{\text{marg}, s}$ with $l \in \{1, \dots, L_{t_s, s}\}$ the function $\hat{\hat{m}}_{t_s}^s$ is a marginal estimator defined by $\hat{\hat{m}}_t^s(x_t) = \frac{1}{n|\mathcal{I}_{t, l}^s|_n} \sum_{X_i \in \mathcal{I}_{t, l}^s} Y_i$. Furthermore we define the density estimator $\hat{p}_t^s(x_t) = |\mathcal{I}_{t, l}^s|_n / |\mathcal{I}_{t, l}^s|$ for $x \in \mathcal{I}_{t, l}^s$ and the $|t \cup t'|$ -dimensional estimator $\hat{p}_{t \cup t'}^s(x_{t \cup t'}) = |\mathcal{I}_{t, l}^s \cap \mathcal{I}_{t', l'}^s|_n / |\mathcal{I}_{t, l}^s \cap \mathcal{I}_{t', l'}^s|$

$\mathcal{I}_{t',l}^s$ for $x \in \mathcal{I}_{t,l}^s \cap \mathcal{I}_{t',l}^s$. With this notation we get

$$\hat{m}_{t_s}^s(x_{t_s}) = \hat{m}_{t_s}^s(x_{t_s}) - \sum_{t \in T_r, t \neq t_s} \int_{(0,1]^{|t \setminus t_s|}} \frac{\hat{p}_{t_s,t}^s(x_{t_s}, u_{t \setminus t_s})}{\hat{p}_{t_s}^s(x_{t_s})} \hat{m}_t^{s-1}(x_{t \cap t_s}, u_{t \setminus t_s}) du_{t \setminus t_s}. \quad (5)$$

Here and in the following, we sometimes write $f(x)$ instead of $f(x_t)$ for functions f that depend only on x via x_t , e.g. $\hat{m}_t^{s-1}(x) = \hat{m}_t^{s-1}(x_t)$. For $t \neq t_s$ we set $\hat{m}_t^s = \hat{m}_t^{s-1}$. After S (S corresponds to `nsplits`) steps we get the estimators \hat{m}_t^S for $t \in T_r$. These estimators are not calibrated in the sense that we do not have $\sum_{i=1}^n \hat{m}_t^S(X_{t \setminus t'}^i, x_{t'}) = 0$ for $t' \subsetneq t$ and $x_{t'} \in [0, 1]^{|t'|}$. Calibration can be achieved by straight forward modifications of \hat{m}_t^S which may require further splits of rectangles $\mathcal{I}_{t',l}^S$ for $t' \subsetneq t$. This will not be discussed here.

Now, the tree family estimator of the function m^0 is given by $\hat{m}^S(x) = \sum_{t \in T_r} \hat{m}_t^S(x_t)$. For the forest estimator, tree family estimators are repeatedly constructed. They are denoted by $\hat{m}_t^{S,v}$ for $t \in T_r$ and $\hat{m}^{S,v}$ for $v = 1, \dots, V$ (V corresponds to `ntrees`). We define the forest estimator as $\hat{m}_t = V^{-1} \sum_{v=1}^V \hat{m}_t^{S,v}$ for $t \in T_r$ and $\hat{m} = V^{-1} \sum_{v=1}^V \hat{m}^{S,v}$. If necessary, we will also write $\mathcal{I}_{t,l}^{s,v}$, $a_{t,k,l}^{s,v}$, t_s^v, k_s^v, \dots instead of $\mathcal{I}_{t,l}^s$, $a_{t,k,l}^s$, t_s, k_s, \dots to indicate that we discuss the tree family estimator with index v .

Considering the above, there are three further modifications in the theoretical version of the algorithm studied in this section compared to the algorithm of the preceding sections. First, we construct trees based on the full sample and not on bootstrap samples. We will see that bootstrap is necessary neither for rate optimality for $r \leq 2$ nor rate improvement by averaging tree families. Our results can be generalized to versions that make use of bootstrap. Second, each tree in a family is grown from an own root. Higher order trees do not come from lower order ones. This assumption is made to simplify mathematical theory. Third, in the iteration steps we make an update of the estimator $\hat{m}_{t_s}^s(x)$ for all rectangles $\mathcal{I}_{t_s,l}^s$ ($l = 1, \dots, L_{t_s,s}$) of the chosen tree t_s . In our implementation of rpf in the preceding

sections we only did this for the splitted rectangle, i.e. for $l = l_s$ and $l = L_{t_s, s}$. From simulations, we concluded that the third change is not severe. For our result, we make use of the following assumptions.

Assumption (A1) The tuples (X_i, ε_i) are i.i.d. The functions $m_t^0 : [0, 1]^{|t|} \rightarrow \mathbb{R}$ are twice continuously differentiable and $E[m_t^0(X_{i,t})] = 0$ for all $t \in T_r$. The covariable X_i has a density p that is bounded from above and below (away from 0). For $t \in T_{2r}$, the joint density p_t of the tuple $X_{i,t}$ allows continuous derivatives of order 2. Conditionally on X_i and the iterative constructions of the leaves in the trees, the error variables ε_i have mean zero and variance bounded by a constant and the products $\varepsilon_i \varepsilon_j$ are mean zero for $i \neq j$. Conditionally on X_i , the iterative constructions of the leaves in the tree families are i.i.d. for $v = 1, \dots, V$.

Assumption (A2) The number S of iterations in the tree family construction and the number V of constructed trees is allowed to depend on n .

Note that S is of the same order as the number of rectangles in the final partition. S is assumed to converge to infinity, see (A3). When considering the forest estimator one usually requires V to converge to infinity in order to obtain useful convergence rates, see also (A7),(A8).

Assumption (A3) For $C_{A3} > 0$ large enough we assume that there exists a constant $C'_{A3} > 0$ such that, with probability tending to one, for $\{s : S - J' \leq s \leq S\}$ and $1 \leq v \leq V$ there exist a partition $S - J' = s_0^v < s_1^v < \dots < s_J^v = S$ such that for $1 \leq j \leq J$ the set $\{t_s^v : s_{j-1}^v < s \leq s_j^v\}$ contains all elements of T_r . Here J and J' are the smallest integers larger or equal to $C_{A3} \log n$ or $C'_{A3}(\log n)^2$, respectively.

Assumption (A4) For $x \in [0, 1]$, $t \in T_r$, $1 \leq v \leq V$ we define $l_t(x) = l_t^v(x)$ such that $x \in \mathcal{I}_{t, l_t^v}^{S, v}$. We assume that with probability tending to one uniformly over $t \in T_r$, $1 \leq v \leq V$, $k \in t$,

$$\frac{1}{n} \sum_{i=1}^n \left(b_{t, k, l_t^v}^{S, v}(X_{i, t}) - a_{t, k, l_t^v}^{S, v}(X_{i, t}) \right)^2 \leq \delta_{1, n}^2$$

for a sequence $\delta_{1, n}$ with $(\log n)^2 \delta_{1, n} \rightarrow 0$ and $n^R \delta_{1, n} \rightarrow \infty$ for $R > 0$ large enough.

Assumption (A5) It holds for $t, t' \in T_r$, $1 \leq v \leq V$ and $S - J' \leq s \leq S$ that

$$\begin{aligned} \sup_{t, t' \in T_r, t \neq t'} \int_{(0, 1]^{|t \cup t'|}} \left(\frac{\widehat{p}_{t \cup t'}^{S, v}(u)}{\widehat{p}_t^{S, v}(u_t)} - \frac{\widehat{p}_{t \cup t'}^{s, v}(u)}{\widehat{p}_t^{s, v}(u_t)} \right)^2 du_{t \cup t'} &\leq \delta_{1, n}^2 (\log n)^{-4}, \\ \sup_{t \in T_r} \int_{(0, 1]^{|t|}} \left(\widehat{m}_t^{S, v}(u_t) - \widehat{m}_t^{s, v}(u_t) \right)^2 du_t &\leq \delta_{1, n}^2 (\log n)^{-4} \end{aligned}$$

with probability tending to one.

Assumption (A6) It holds uniformly for $t, t' \in T_r$, $1 \leq v \leq V$ that

$$\begin{aligned} \int_{(0, 1]^{|t \cup t'|}} \left(\frac{\widehat{p}_{t \cup t'}^{S, v}(u)}{\widehat{p}_t^{S, v}(u_t)} - \frac{p_{t \cup t'}(u)}{p_t(u_t)} \right)^2 du_{t \cup t'} &\leq \delta_{2, n}^2, \\ \sup_{u \in (0, 1]^{|t|}} |\widehat{p}_t^{s, v}(u) - p_t(u)| &\leq \eta_{1, n} \text{ for } s = S, S - J' - 1, \end{aligned}$$

with probability tending to one for sequences $\delta_{2, n}$, $\eta_{1, n}$ with $(\log n)^2 \delta_{2, n} \rightarrow 0$ and $\eta_{1, n} \rightarrow 0$.

Theorem 5.1. Under (A1)–(A6), for $1 \leq v \leq V$ the tree family estimators satisfy

$$\left\| \sum_{t \in T_r} (\widehat{m}_t^{S, v} - m_t^0) \right\| = O_P(\delta_{1, n} + S^{1/2} n^{-1/2})$$

with probability tending to one, where $\|\cdot\|$ denotes the $L_2(P)$ norm.

We shortly discuss this result. Suppose that the rectangles $\mathcal{I}_{t,l}^s$ have side lengths of order h for some sequence $h \rightarrow 0$. Then $\delta_{1,n}$ is of order h , S is of order h^{-r} and up to logarithmic terms we obtain a rate of order $h + (nh^r)^{-1/2}$ for the estimation error of $\hat{m}^{S,v} = \sum_{t \in T_r} \hat{m}_t^{S,v}$. For discussing the complete forest estimator, we need the following assumptions.

Assumption (A7) It holds uniformly for $t, t' \in T_r$, $1 \leq v \leq V$ that

$$\begin{aligned} \sup_{u \in (0,1]^{|t \cup t'|}} \left| \hat{p}_{t \cup t'}^{S,v}(u) - p_{t \cup t'}(u) \right| &\leq \eta_{2,n}, \\ \|\hat{p}_t^{S,v} - p_t(u)\|, \left\| \int_{(0,1]^{|t' \setminus t|}} \frac{\hat{p}_{t \cup t'}^{S,v}(u) - p_{t \cup t'}(u)}{p_t(u)} m_{t'}^0(u_{t'}) du_{t' \setminus t} \right\| &\leq \delta_{3,n} \end{aligned}$$

with probability tending to one for some sequences $\eta_{2,n}, \delta_{3,n}$ with $\eta_{2,n}, \delta_{3,n} \rightarrow 0$.

Assumption (A8) For $t, t' \in T_r$ we write $\hat{p}_{t \cup t'}^{S,+} = V^{-1} \sum_{v=1}^V \hat{p}_{t \cup t'}^{S,v}$ and $\hat{p}_t^{S,+} = V^{-1} \sum_{v=1}^V \hat{p}_t^{S,v}$.

It holds uniformly for $t, t' \in T_r$ that

$$\|\hat{p}_t^{S,+} - p_t(u)\|_1, \left\| \int_{(0,1]^{|t' \setminus t|}} \frac{\hat{p}_{t \cup t'}^{S,+}(u) - p_{t \cup t'}(u)}{p_t(u)} m_{t'}^0(u_{t'}) du_{t' \setminus t} \right\|_1 \leq \delta_{4,n}$$

with probability tending to one for a sequence $\delta_{4,n} \rightarrow 0$. Here, $\|\cdot\|_1$ denotes the $L_1(P)$ norm.

Below we will argue that under certain assumptions the averaged estimators in (A8) can achieve rates of convergence $\delta_{4,n} = O(\delta_{1,n}^2)$, compared to their summands which have a bias of order $\delta_{1,n}$. If the density p_t is twice continuously differentiable, qualitatively, $\hat{p}_t^{S,+}$ behaves like a kernel density estimator with bandwidth h of order $\delta_{1,n}$. We switch from the $L_2(P)$ norm to the $L_1(P)$ norm in Assumption (A8) and in the next theorem, because at the boundary of size Ch with C large enough we have a bias of order h and in the interior the bias is of order h^2 . Thus, measured by the $L_1(P)$ norm we get a bias of order

h^2 whereas the $L_2(P)$ -norm has a slower rate caused by the boundary effects.

Theorem 5.2. *Under (A1)–(A8), for the forest estimator we have*

$$\left\| \sum_{t \in T_r} (\hat{m}_t - m_t^0) \right\|_1 \leq C(\delta_{1,n}^2 + \delta_{1,n}\delta_{2,n} + \delta_{3,n}^2 + \delta_{4,n} + S^{1/2}n^{-1/2})$$

with probability tending to one.

Again, we shortly discuss this result. As above, suppose that the rectangles $\mathcal{I}_{t,l}^s$ have side lengths of order h for some sequence $h \rightarrow 0$. Then $\delta_{1,n}$ is of order h and S is of order h^{-r} . The sequence $\delta_{2,n}$ is the rate of a histogram estimator of dimension $\leq 2r$ which up to logarithmic terms is of order $h + (nh^{2r})^{-1/2}$ for $2r$ dimensional estimators. Assume for $x \in [0, 1]^{|t|}$ sufficiently far away from the boundary of $[0, 1]^{|t|}$ the random variables $x_k - a_k^S$ and $b_k^S - x_k$ approximately follow the same distribution, where a_k^S, b_k^S are the lower and upper bounds of the leaf which contains x with respect to dimension k . Then the bias terms of order h cancel and we get that the bias terms measured by $\delta_{4,n}$ are of order h^2 . Thus up to logarithmic terms, we get a bound on the accuracy of the forest estimator of order $h^2 + h(nh^{2r})^{-1/2} + (nh^r)^{-1/2}$. This rate is faster than the tree family rate if $nh^{2r} \rightarrow \infty$, i.e. we need consistency of $2r$ dimensional histogram estimators. These histogram estimators show up as kernels in integral equations which define the tree family and forest estimator. This means that, approximately, the tree family estimators \hat{m}^v are given as solutions of integral equations of the form $\hat{m}^v = \bar{m}^v + A^v \hat{m}^v$ with random integral operators A^v , where the operators A^v are defined by up to $2r$ dimensional density estimators. If these density estimators are consistent the operators A^v are approximately equal to an operator A not depending of v . Then, \hat{m}^v approximately solves $\hat{m}^v = \bar{m}^v + A\hat{m}^v$ and the forest estimator $\hat{m} = V^{-1} \sum_{v=1}^V \hat{m}^v$ solves approximately $\hat{m} = V^{-1} \sum_{v=1}^V \bar{m}^v + A\hat{m}$. For getting faster

convergence rates for the forest estimator one shows that the average $V^{-1} \sum_{v=1}^V \bar{m}^v$ has faster rates as the summands \bar{m}^v . For the whole argument it is crucial that up to $2r$ dimensional density estimators are consistent. Also in case these estimators are inconsistent we expect a better performance of forest estimators compared to tree family estimators. However, additional terms show up in the expansion of the rpf estimator that are not of order h^2 . Let us discuss this for a bandwidth h that is rate optimal for dimension r when one estimates r dimensional twice differentiable functions. Then h is of order $n^{-1/(r+4)}$ and the $2r$ -dimensional estimators are consistent only for $r \leq 3$. Thus our result shows that for optimal tuning parameters forest estimators perform better as tree family estimators for $r \leq 3$. For $r \leq 2$ we obtain optimal rates by the forest estimator, i.e. $n^{-2/5}$ for $r = 1$ and $n^{-1/3}$ for $r = 2$.

Note that our results also hold for other iterative partition schemes as long as Assumptions (A1)–(A8) are fulfilled. In particular, in the proofs we did not use that partitions are based on iterative splitting as described in the first part of this section.

6 Conclusion

We introduce a new tree based prediction method coined random planted forest. While fully flexible, it follows a structured path by growing trees in a family simultaneously which approximate terms of a functional decomposition. A first simulation study provided in this paper shows promising results. Rpf seems to be able to detect both jumps in the regression function as well as interactions between predictors. Especially in sparse settings, rpf demonstrated an unmatched combination of accuracy and flexibility under easily interpretable models. Rpf predictions are easily visualisable if the maximal order of interaction of the estimator is bounded by either one or two.

References

- Agarwal, R., N. Frosst, X. Zhang, R. Caruana, and G. E. Hinton (2020). Neural additive models: Interpretable machine learning with neural nets. *arXiv preprint arXiv:2004.13912*, 1–17.
- Apley, D. W. and J. Zhu (2020). Visualizing the effects of predictor variables in black box supervised learning models. *Journal of the Royal Statistical Society: Series B (Statistical Methodology)* 82(4), 1059–1086.
- Biau, G. (2012). Analysis of a random forests model. *The Journal of Machine Learning Research* 13(1), 1063–1095.
- Biau, G., L. Devroye, and G. Lugosi (2008). Consistency of random forests and other averaging classifiers. *Journal of Machine Learning Research* 9(Sep), 2015–2033.
- Biau, G. and E. Scornet (2016). A random forest guided tour. *Test* 25(2), 197–227.
- Breiman, L. (2001). Random forests. *Machine learning* 45(1), 5–32.
- Breiman, L. and J. H. Friedman (1985). Estimating optimal transformations for multiple regression and correlation. *Journal of the American statistical Association* 80(391), 580–598.
- Buja, A., T. Hastie, and R. Tibshirani (1989). Linear smoothers and additive models. *The Annals of Statistics* 17(2), 453–510.
- Caruana, R., Y. Lou, J. Gehrke, P. Koch, M. Sturm, and N. Elhadad (2015). Intelligible models for healthcare: Predicting pneumonia risk and hospital 30-day readmission. In *Proceedings of the 21th ACM SIGKDD international conference on knowledge discovery and data mining*, pp. 1721–1730.

- Chastaing, G., F. Gamboa, C. Prieur, et al. (2012). Generalized hoeffding-sobol decomposition for dependent variables-application to sensitivity analysis. *Electronic Journal of Statistics* 6(2012), 2420–2448.
- Chen, T. and C. Guestrin (2016). Xgboost: A scalable tree boosting system. In *Proceedings of the 22nd acm sigkdd international conference on knowledge discovery and data mining*, pp. 785–794.
- Chen, T., T. He, M. Benesty, V. Khotilovich, Y. Tang, H. Cho, K. Chen, R. Mitchell, I. Cano, T. Zhou, M. Li, J. Xie, M. Lin, Y. Geng, and Y. Li (2020). xgboost: Extreme gradient boosting. R package version 1.2.0.1.
- Chipman, H. A., E. I. George, and R. E. McCulloch (2010). Bart: Bayesian additive regression trees. *The Annals of Applied Statistics* 4(1), 266–298.
- Collobert, R., J. Weston, L. Bottou, M. Karlen, K. Kavukcuoglu, and P. Kuksa (2011). Natural language processing (almost) from scratch. *Journal of machine learning research* 12(ARTICLE), 2493–2537.
- Friedman, J. H. (1991). Multivariate adaptive regression splines. *The annals of statistics* 19(1), 1–67.
- Friedman, J. H. (2001). Greedy function approximation: a gradient boosting machine. *Annals of statistics* 29(5), 1189–1232.
- Friedman, J. H. and W. Stuetzle (1981). Projection pursuit regression. *Journal of the American statistical Association* 76(376), 817–823.
- Geurts, P., D. Ernst, and L. Wehenkel (2006). Extremely randomized trees. *Machine learning* 63(1), 3–42.

- Grinsztajn, L., E. Oyallon, and G. Varoquaux (2022). Why do tree-based models still outperform deep learning on typical tabular data? In *Thirty-sixth Conference on Neural Information Processing Systems Datasets and Benchmarks Track*.
- Hastie, M. T. (2020). Package ‘mda’.
- Hinton, G., L. Deng, D. Yu, G. E. Dahl, A.-r. Mohamed, N. Jaitly, A. Senior, V. Vanhoucke, P. Nguyen, T. N. Sainath, et al. (2012). Deep neural networks for acoustic modeling in speech recognition: The shared views of four research groups. *IEEE Signal processing magazine* 29(6), 82–97.
- Hofner, B., A. Mayr, N. Robinzonov, and M. Schmid (2014). Model-based boosting in r: a hands-on tutorial using the r package mboost. *Computational statistics* 29(1), 3–35.
- Hooker, G. (2007). Generalized functional anova diagnostics for high-dimensional functions of dependent variables. *Journal of Computational and Graphical Statistics* 16(3), 709–732.
- LeCun, Y., Y. Bengio, and G. Hinton (2015). Deep learning. *nature* 521(7553), 436–444.
- Lengerich, B., S. Tan, C.-H. Chang, G. Hooker, and R. Caruana (2020). Purifying interaction effects with the functional anova: An efficient algorithm for recovering identifiable additive models. In *International Conference on Artificial Intelligence and Statistics*, pp. 2402–2412. PMLR.
- Lou, Y., R. Caruana, and J. Gehrke (2012). Intelligible models for classification and regression. In *Proceedings of the 18th ACM SIGKDD international conference on Knowledge discovery and data mining*, pp. 150–158.

- Lou, Y., R. Caruana, J. Gehrke, and G. Hooker (2013). Accurate intelligible models with pairwise interactions. In *Proceedings of the 19th ACM SIGKDD international conference on Knowledge discovery and data mining*, pp. 623–631.
- Mentch, L. and G. Hooker (2016). Quantifying uncertainty in random forests via confidence intervals and hypothesis tests. *The Journal of Machine Learning Research* 17(1), 841–881.
- Mentch, L. and G. Hooker (2017). Formal hypothesis tests for additive structure in random forests. *Journal of Computational and Graphical Statistics* 26(3), 589–597.
- Nelder, J. A. and R. W. Wedderburn (1972). Generalized linear models. *Journal of the Royal Statistical Society: Series A (General)* 135(3), 370–384.
- Nielsen, J. P. and S. Sperlich (2005). Smooth backfitting in practice. *Journal of the Royal Statistical Society: Series B (Statistical Methodology)* 67(1), 43–61.
- Peng, W., T. Coleman, and L. Mentch (2019). Asymptotic distributions and rates of convergence for random forests via generalized u-statistics. *arXiv preprint arXiv:1905.10651 Preprint*, 1–62.
- Rawat, W. and Z. Wang (2017). Deep convolutional neural networks for image classification: A comprehensive review. *Neural computation* 29(9), 2352–2449.
- Scornet, E., G. Biau, J.-P. Vert, et al. (2015). Consistency of random forests. *The Annals of Statistics* 43(4), 1716–1741.
- Sparapani, R., C. Spanbauer, and R. McCulloch (2021). Nonparametric machine learning and efficient computation with bayesian additive regression trees: the bart r package. *Journal of Statistical Software* 97(1), 1–66.

- Stone, C. J. (1994). The use of polynomial splines and their tensor products in multivariate function estimation. *The Annals of Statistics* 22(1), 118–171.
- Tan, Y. S., A. Agarwal, and B. Yu (2022). A cautionary tale on fitting decision trees to data from additive models: generalization lower bounds. In *International Conference on Artificial Intelligence and Statistics*, pp. 9663–9685. PMLR.
- Tan, Y. S., C. Singh, K. Nasseri, A. Agarwal, and B. Yu (2022). Fast interpretable greedy-tree sums (figs). *arXiv preprint arXiv:2201.11931*.
- Wager, S. and S. Athey (2018). Estimation and inference of heterogeneous treatment effects using random forests. *Journal of the American Statistical Association* 113(523), 1228–1242.
- Wood, S. N. (2011). Fast stable restricted maximum likelihood and marginal likelihood estimation of semiparametric generalized linear models. *Journal of the Royal Statistical Society: Series B (Statistical Methodology)* 73(1), 3–36.
- Wright, M. N. and A. Ziegler (2015). ranger: A fast implementation of random forests for high dimensional data in c++ and r. *arXiv preprint arXiv:1508.04409*.

A The Random Planted Forest Algorithm

In this section, we add some technical details which improve the understanding of this paper. We first give a short overview over the algorithm in the additive case, i.e. if $r = 1$. The simplification is easier to understand and is of particular interest in our simulation studies in Section 4. Next, we include the discussion of an identification constraint for the functional decomposition, which is important for plotting the components. Lastly, we add some additional remarks.

A.1 Additive Random Planted Forests

In this section, we explain the rpf algorithm in the additive case. Thus, we assume that m has an additive structure

$$m(x) = m_{\emptyset} + m_1(x_1) + \cdots + m_d(x_d).$$

The algorithm then simplifies in the following way. The algorithm now grows a tree for each coordinate $k \in \{1, \dots, d\}$. As discussed above, the tree $t = \emptyset$ never grows during the algorithm. Thus, in every step, a coordinate k is chosen for which the tree k is grown. Furthermore, the set V_r introduced in Subsection 2.3 reduces to

$$V = \{(k, \{k\}) \mid k \in \{1, \dots, d\}\}.$$

In particular, it does not depend on the current state of the family of planted trees. Noting that $|V| = d$, the value $\mathbf{m_try} := \lceil \mathbf{t_try} \cdot d \rceil$ is constant throughout the algorithm. The parameter $\mathbf{t_try}$ or equivalently $\mathbf{m_try}$ act exactly the same as the parameter $\mathbf{m_try}$ in Breimans implementation of random forests. In this case, the algorithms mainly differ due

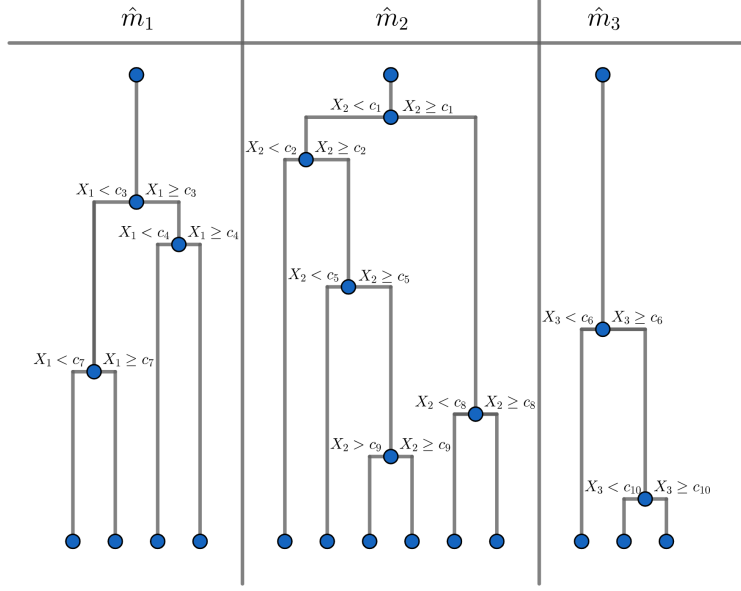


Figure 5: Illustration of an additive family of planted trees. Trees grow simultaneously and the height of an edge indicates when the split occurred.

to the fact that instead of growing a single tree including all coordinates, the rpf algorithm grows a tree for each coordinate separately.

An illustration of the construction of a family of additive planted trees is given in Figure 5. Observe that in this case the leaves of a tree form a partition of \mathbb{R} . Each data point is contained in exactly one leaf of each tree. Note that the latter two statements do not hold in general in the additive case.

A.2 Identification Constraint

If $r \in \{1, 2\}$, the components can be visualised easily. In order to reasonably compare plots, we need a condition that ensures uniqueness of the functional decomposition. We

assume that for every $u \subseteq \{1, \dots, d\}$ and $k \in u$,

$$\int m_u(x_u) \int w(x) dx_{-u} dx_k = 0, \quad (6)$$

for some weight function w . With this constrained the decomposition is known as generalized functional ANOVA. Observe that this is not an additional assumption on the overall function m . The constraint ensures that the functional decomposition is unique for non-degenerated cases. One possibility is $w(x) = \prod_k \hat{p}_k(x_k)$, where \hat{p}_k is an estimate of the marginal density of the design density of X . The resulting plots are known as partial dependence plots (Friedman, 2001). With the burden of extra computational cost, one can choose w as an estimate of the full design density, see also Lengerich et al. (2020). Compared to the previous example, a computationally more efficient constraint has recently been proposed in Apley and Zhu (2020). Depending on the viewpoint, different choices for w may be advantageous. Since the precise constraint is not the focus of this paper, we settled for the simple constraint $w \equiv 1$ which suffices in the sense that it allows us to compare plots of different estimators.

Note that while we obtain a tree for every component in the ANOVA decomposition (except the constant), in general, these estimators do not satisfy the constraint (6). Thus, in order to obtain suitable estimators for the components, we must normalize the estimated components without changing the overall estimator. This can be achieved by using an algorithm similar to the purification algorithm given in Lengerich et al. (2020).

A.3 Additional Remarks

This subsection contains various remarks to further enhance the understanding of the algorithm.

As for the backfitting algorithm (Breiman and Friedman, 1985), updating the estimator in each iteration step is important, especially when the predictors are correlated. We also considered alternative updating procedures such as updating all leaves in the tree where the split occurs. While this may be worth some consideration, we observed the best results with our current version. Secondly, we impose 3 conditions that must be satisfied for a split to be viable. The first condition (C_1) is obviously required, since we need a leaf to split. The second condition is necessary in order to assure that the resulting trees are elements of T_r - we do not want leaves of trees to depend on more than r coordinates. We impose (C_3) so that each leaf contains at least 1 observation. Also, note that the tree $t = \emptyset$ never grows during the algorithm. Rather, it functions as the root leaf of the trees t with $|t| = 1$. This implies $\hat{m}_{\emptyset} = 0$ throughout the algorithm.

Besides interpretability, advantages of restricting the order of approximation in the ANOVA expansion (2) are potentially faster convergence rates as well as the possibility of using more constrained estimators. In the simulation study in Section 4, we find that using an unconstrained rpf works surprisingly well, even if the data generating regression function is additive, i.e. a first order approximation is exact. A constrained version slightly improves the results. The flexibility, however, comes with the cost of reduced interpretability.

B Proofs

Proof of Theorem 5.1 In the proof we denote different constants by C . The meaning of C may change, also in the same formula. In this proof we omit the index v in the notation.

We rewrite (5) as

$$\widehat{m}^s(x) = \widehat{m}^s(x_{t_s}) + \widehat{\Psi}^s \widehat{m}^{s-1}(x), \quad (7)$$

where $\widehat{m}^s = \widehat{m}_{t_s}^s$, $\widehat{\Psi}^s = \widehat{\Psi}_{t_s}^s$ and where

$$\begin{aligned} \widehat{\Psi}_t^s m(x) &= m(x) - m_t(x_t) \\ &\quad - \sum_{t' \in T_r, t' \neq t} \int_{(0,1]^{|t' \setminus t|}} \frac{\widehat{p}_{t \cup t'}^s(x_t, u_{t' \setminus t})}{\widehat{p}_t^s(x_t)} m_{t'}(x_{t' \cap t}, u_{t' \setminus t}) du_{t' \setminus t} \end{aligned}$$

for an additive function $m(x) = \sum_{t \in T_r} m_t(x_t)$. Iterative application of (7) gives for $1 \leq$

$$S_1 < S_2 \leq S$$

$$\begin{aligned} \widehat{m}^{S_2} &= \widehat{m}^{S_2} + \widehat{\Psi}^{S_2} \widehat{m}^{S_2-1} + \widehat{\Psi}^{S_2} \widehat{\Psi}^{S_2-1} \widehat{m}^{S_2-2} \\ &\quad + \dots + \widehat{\Psi}^{S_2} \dots \widehat{\Psi}^{S_1+1} \widehat{m}^{S_1} + \widehat{\Psi}^{S_2} \dots \widehat{\Psi}^{S_1} \widehat{m}^{S_1-1}. \end{aligned} \quad (8)$$

We will use this equality in the proofs of the following lemmas for the choices $S_1 = 1, S_2 = S^*$ and $S_1 = S^*, S_2 = S$ with $S^* = S - J'$.

Lemma B.1. *It holds that*

$$\frac{1}{n} \sum_{i=1}^n \widehat{m}^{S^*-1}(X_i)^2 \leq S^{1/2} \frac{1}{n} \sum_{i=1}^n Y_i^2.$$

Proof. It can be easily shown that for $t \in T_r$

$$\frac{1}{n} \sum_{i=1}^n \widehat{m}_t(X_i)^2 \leq \frac{1}{n} \sum_{i=1}^n Y_i^2. \quad (9)$$

Furthermore, for any function m we have

$$\frac{1}{n} \sum_{i=1}^n \left(\widehat{\Psi}^s m \right) (X_i)^2 \leq \frac{1}{n} \sum_{i=1}^n m(X_i)^2. \quad (10)$$

For a proof of (10) consider the space of functions $m : [0, 1]^d \rightarrow \mathbb{R}$ endowed with the pseudo metric

$$\|m\|_{n,2}^2 = \frac{1}{n} \sum_{i=1}^n m(X_i)^2.$$

Then $I - \widehat{\Psi}^s$ is the orthogonal projection onto the space of piecewise constant functions that are constant on the rectangles $\mathcal{I}_{t,l}^s : l = 1, \dots, L_{t,s}$. Furthermore, $\widehat{\Psi}^s$ is the orthogonal projection onto the orthogonal complement of this space. This shows (10). The statement of the lemma now follows from (9)–(10) by application of (8) with $S_1 = 1$ and $S_2 = S^* - 1$. \square

This lemma can be used to show a bound for the $L_2(p)$ -norm of \widehat{m}^{S^*-1} which we denote by $\|\widehat{m}^{S^*-1}\|$

Lemma B.2. *It holds that with probability tending to one*

$$\|\widehat{m}^{S^*-1}\|^2 = \int \widehat{m}^{S^*-1}(x)^2 p(x) dx \leq (1 - C\eta_{1,n})^{-1} S^{1/2} \frac{1}{n} \sum_{i=1}^n Y_i^2.$$

Proof. For $t \in T_r$ we get by application of (A6) that

$$\begin{aligned} \int \widehat{m}_t^{S^*-1}(x_t)^2 p(x) dx &\leq \int \widehat{m}_t^{S^*-1}(x_t)^2 \widehat{p}_t^{S^*-1}(x_t) dx_t \\ &\quad + \int \widehat{m}_t^{S^*-1}(x_t)^2 |\widehat{p}_t^{S^*-1} - p_t|(x_t) dx_t \\ &\leq \frac{1}{n} \sum_{i=1}^n \widehat{m}_t^{S^*-1}(X_{t,i})^2 \\ &\quad + C\eta_{1,n} \int \widehat{m}_t^{S^*-1}(x_t)^2 p_t(x_t) dx_t. \end{aligned}$$

The statement of the lemma now follows by application of Lemma B.1. \square

Lemma B.3. *It holds for some $C > 0$ and $0 < \rho < 1$ that with probability tending to one*

$$\|\widehat{\Psi}^S \circ \dots \circ \widehat{\Psi}^{S^*}\| \leq C\rho^{C_{A3} \log n}.$$

Here for an operator Ψ mapping $L_2(p)$ into $L_2(p)$ we denote the operator norm $\|\Psi\| = \sup\{\|\Psi m\| : m \in L_2(p), \|m\| = 1\}$ by $\|\Psi\|$. Before we come to the proof of this lemma let us discuss its implications. Using the representation (7) we get from Lemmas B.2, B.3 that for all $R > 0$ we can choose a constant C_R such that if C_{A3} is large enough with probability tending to one

$$\|\widehat{m}^S - \widehat{m}^{1,S}\| \leq C_R n^{-R}, \tag{11}$$

where

$$\widehat{m}^{1,S} = \widehat{m}^S + \widehat{\Psi}^S \widehat{m}^{S-1} + \dots + \widehat{\Psi}^S \dots \widehat{\Psi}^{S^*+1} \widehat{m}^{S^*}.$$

Note that $\widehat{m}^{1,S}$ only depends on the growth history of the tree in the last $C'_J(\log n)^2$ steps. Thus we have shown that approximately the same holds for the tree estimators \widehat{m}^S . Below we will go a step further and show that the tree family estimator approximately only depends on the data averages in the terminal leaves and in particular not on the growth of the tree family in the past. Before we come to this refinement we first give a proof of Lemma B.3. For this purpose we will introduce population analogues Ψ_{t_s} of the operators $\widehat{\Psi}^s$ and we will discuss some theory on backfitting estimators in additive interaction models. We consider the following subspaces of functions $m : [0, 1]^d \rightarrow \mathbb{R}$ with $E[m^2(X_i)] < \infty$ for

$$t \in T_r$$

$$\mathcal{H} = \{m : [0, 1]^d \rightarrow \mathbb{R} \mid E[m^2(X_i)] < \infty\},$$

$$\mathcal{H}_t = \{m \in \mathcal{H} \mid m(x) = m_t(x_t) \text{ for some function } m_t : [0, 1]^{|t|} \rightarrow \mathbb{R}\},$$

$$\begin{aligned} \mathcal{H}_{add} = \{m \in \mathcal{H} \mid m(x) = \sum_{t \in T_r} m_t(x_t) \text{ for some functions} \\ m_t \in \mathcal{H}_t, t \in T_r\}. \end{aligned}$$

In particular, \mathcal{H}_\emptyset is the subspace of \mathcal{H} that contains only constant functions. In abuse of notation for a function $m_t \in \mathcal{H}_t$ we also write $m_t(x)$ with $x \in [0, 1]^d$ instead of $m_t(x_t)$. Thus m_t can be interpreted as a function with domain $[0, 1]^{|t|}$ or with domain $[0, 1]^d$. The projection of \mathcal{H} onto \mathcal{H}_t is denoted by Π_t . For $\Psi_t = I - \Pi_t$ and $m = \sum_{t \in T_r} m_t$ with $m_t \in \mathcal{H}_t$ ($t \in T_r$) one gets

$$\Psi_t m(x) = \sum_{w \in T_r \setminus \{t\}} m_w(x_w) + m_t^*(x_t)$$

with

$$m_t^*(x_t) = - \sum_{w \in T_r, w \neq t} \int \frac{p_{t \cup w}(x_{t \cup w})}{p_t(x_t)} m_w(x_w) dx_{w \setminus t}.$$

We now consider operators K of the form $\Psi_{t^1} \circ \dots \circ \Psi_{t^{k_K}}$ with $\{t^1, \dots, t^{k_K}\} \supseteq T_r$. We call these operators complete. We argue that there exists a constant $\gamma < 1$ such that for all complete operators K of this form we have

$$\|K\|_{add} = \sup\{\|Km\| : m \in \mathcal{H}_{add}, \|m\| \leq 1\} < \gamma. \quad (12)$$

Note that in particular γ does not depend on the order of t^1, \dots, t^{k_K} . Our notation is a little bit sloppy because in the representation $\sum_{t \in T_r} m_t$ of m the summands are not uniquely defined because $t \cap t'$ may be nonempty for some $t, t' \in T_r$, $t \neq t'$. A more appropriate

notation would be to define K as an operator mapping $\prod_{t \in T_r} \mathcal{H}_t$ into $\prod_{t \in T_r} \mathcal{H}_t$ and to endow this space with the pseudo norm $\|\sum_{t \in T_r} m_t\|$. For a proof of (12) we will show that $\sum_{t \in T} \mathcal{H}_t$ are closed subspaces of \mathcal{H} for all choices of $T \subset T_r$. In particular, by a result of Deutsch (1985), see also Appendix A.4 in Bickel, Klaassen, Ritov and Wellner (1993), this implies that $\rho(\mathcal{H}_{t_j}, \mathcal{H}_{t_{j+1}} + \dots + \mathcal{H}_{t_{k_K}}) < 1$ for $1 \leq j \leq t_{k_K-1}$, where for two linear subspaces L_1 and L_2 of \mathcal{H} the quantity $\rho(L_1, L_2)$ is the cosine of the minimal angle between L_1 and L_2 , i.e. $\rho(L_1, L_2) = \sup\{\int h_1(x)h_2(x)p(x)dx : h_j \in L_j \cap (L_1 \cap L_2)^\perp, \int h_j^2(x)p(x)dx \leq 1 \text{ for } j = 1, 2\}$.

According to a result of Smith, Solomon and Wagner (1977) this implies that for an operator K of the above form we have that

$$\|K\|_{add} \leq 1 - \prod_{j=1}^{k_K} \sin^2(\alpha_j),$$

where α_j is chosen such that $\cos(\alpha_j) = \rho(\mathcal{H}_{t_j}, \mathcal{H}_{t_{j+1}} + \dots + \mathcal{H}_{t_{k_K}})$. We remark that this bound is also valid if the space \mathcal{H}_{t_j} is identical to the same space \mathcal{H}_t for several choices of j . In this case we have $\sin^2(\alpha_j) = 1$ for all such values of the index j with the exception of the last appearance of \mathcal{H}_t . Because there are only finitely many ways to order $|T_r|$ elements we get by the last remark that (12) holds with some $\gamma < 1$ for all operators K . For a proof of (12) it remains to show that $\sum_{t \in T} \mathcal{H}_t$ are closed subspaces of \mathcal{H} for all choices of $T \subset T_r$. For this claim we will argue that $\sum_{t \in T} \bar{\mathcal{H}}_t$ are closed subspaces of \mathcal{H} for all choices of $T \subset T_r$, where $\bar{\mathcal{H}}_t = \{h \in \mathcal{H}_t : \int h(x)dx_j = 0 \text{ for } j \in t\}$. According to Proposition 2 in supplement material A.4 of Bickel, Klaassen, Ritov and Wellner (1993) this follows if there exists some $c > 0$ such that $\int (\sum_{t \in T} h_t(x_t))^2 p(x)dx \geq 1$ implies that $\int h_t(x_t)^2 p(x)dx \geq c$ for some $t \in T$. This can be easily verified with $c = C(\max_{x \in [0,1]^d} p(x))^{-1}|T_r|^{-1}$ by noting

that for $h_t \in \bar{\mathcal{H}}_t$ it holds that

$$\begin{aligned}
\int \left(\sum_{t \in T} h_t(x_t) \right)^2 p(x) dx &\leq \max_{x \in [0,1]^d} p(x) \int \left(\sum_{t \in T} h_t(x_t) \right)^2 dx \\
&= \max_{x \in [0,1]^d} p(x) \sum_{t \in T} \int h_t(x_t)^2 dx \\
&\leq C \max_{x \in [0,1]^d} p(x) \sum_{t \in T} \int h_t(x_t)^2 p(x) dx
\end{aligned}$$

In particular, one can use (12) to show that with

$$\bar{m}_t(x) = E[Y_i | X_{i,t} = x_t] = \sum_{t' \in T_r} \int m_{t'}(x_{t'}) \frac{p_{t' \cup t}(x_{t' \cup t})}{p_t(x_t)} dx_{t' \setminus t}$$

we have for $\mu^* \in \mathcal{H}_{add}$ with some $0 < \gamma < 1$, and some $C > 0$

$$\|m - \mu\| \leq C \gamma^{S^*} (\|\mu^*\| + 1),$$

where

$$\mu = \bar{m}_{t_{v,1}^*} + \Psi_{t_{v,1}^*} \bar{m}_{t_{v,2}^*} + \Psi_{t_{v,1}^*} \Psi_{t_{v,2}^*} \bar{m}_{t_{v,3}^*} + \dots + \Psi_{t_{v,1}^*} \circ \dots \circ \Psi_{t_{v,S^*-1}^*} \mu^*$$

with $t_{v,s}^* = t_{v,S-s+1}$. Note that

$$m - \mu = \Psi_{t_{v,1}^*} \circ \dots \circ \Psi_{t_{v,S^*-1}^*} (m - \mu^*).$$

Proof of Lemma B.3. By Assumption (A6) we have by application of Cauchy-Schwarz inequality that

$$\|\hat{\Psi}^s - \Psi_{t_s}\| \leq C \delta_{2,n} \tag{13}$$

with probability tending to one. This implies that, with probability tending to one,

$$\|\widehat{\Psi}^s\| \leq 1 + C\delta_{2,n}$$

and we get by a telescope argument that, with probability tending to one, for $1 \leq j \leq J \leq C_{A3} \log n + 1$

$$\begin{aligned} \|\widehat{\Psi}^{s_j} \circ \dots \circ \widehat{\Psi}^{s_{j-1}+1} - \Psi_{t_{s_j}} \circ \dots \circ \Psi_{t_{s_{j-1}+1}}\| &\leq CJ'(1 + C\delta_{2,n})^{J'-1} \delta_{2,n} \\ &\leq CC'_{A3}(\log n)^2(1 + C\delta_{2,n})^{C'_{A3}(\log n)^2} \delta_{2,n} \leq C(\log n)^2 \delta_{2,n}. \end{aligned}$$

Because by Assumption (A3) $\Psi_{t_{s_j}} \circ \dots \circ \Psi_{t_{s_{j-1}+1}}$ is a complete operator with high probability, we get from (12) that, with probability tending to one, for $1 \leq j \leq J \leq C_{A3} \log n + 1$

$$\|\widehat{\Psi}^{s_j} \circ \dots \circ \widehat{\Psi}^{s_{j-1}+1}\| \leq \gamma + C(\log n)^2 \delta_{2,n}.$$

This inequality can be used to show the bound on $\|\widehat{\Psi}^S \circ \dots \circ \widehat{\Psi}^{S*}\|$, claimed in Lemma B.3. □

As discussed above, Lemma B.3 implies (11). We now approximate $\widehat{m}^{1,S}$ by $\widehat{m}^{2,S}$ where

$$\widehat{m}^{2,S} = \widehat{m}_{t_S}^S + \widehat{\Psi}_{t_S}^S \widehat{m}_{t_{S-1}}^S + \widehat{\Psi}_{t_S}^S \widehat{\Psi}_{t_{S-1}}^S \widehat{m}_{t_{S-2}}^S + \dots + \widehat{\Psi}_{t_S}^S \dots \widehat{\Psi}_{t_{S^*+1}}^S \widehat{m}_{t_{S^*}}^S.$$

Note that $\widehat{m}^{2,S}$ differs from $\widehat{m}^{1,S}$ by having always the superindex S for the operators Ψ and the functions \widehat{m} . In the following lemma we compare \widehat{m}^S and $\widehat{m}^{2,S}$. The bound can be shown by similar arguments as in the proof of (11). In this proof one uses Assumption (A5) instead of (13). One gets that for all $R > 0$ we can choose a constant C_R such that

if C_{A3} in Assumption (A3) is large enough with probability tending to one $\|\widehat{m}^S - \widehat{m}^{2,S}\| \leq C_R n^{-R} + CC'_{A3}(1 + C\delta_{2,n})^{C'_{A3}(\log n)^2} \delta_{1,n} \leq C_R n^{-R} + C\delta_{1,n}$. If R is chosen large enough we get the following lemma, see Assumption (A4).

Lemma B.4. *If C_{A3} in Assumption (A3) is large enough it holds that with probability tending to one*

$$\|\widehat{m}^S - \widehat{m}^{2,S}\| \leq C\delta_{1,n}.$$

We now define $\widehat{m}^{3,S} = \sum_{t \in T_r} \widehat{m}_t^{3,S}$ as a minimizer of

$$\sum_{i=1}^n \left(Y_i - \sum_{t \in T_r} m_t(X_{i,t}) \right)^2$$

over all function $m_t : (0, 1]^{|t|} \rightarrow \mathbb{R}$ that are piecewise constant on the rectangles $\mathcal{I}_{t,l}^S : l = 1, \dots, L_{t,S}$. Then we have $\widehat{\Psi}_t^S \widehat{m}^{3,S} + \widehat{m}_t^S = \widehat{m}^{3,S}$ for all $t \in T_r$ which implies that

$$\widehat{m}^{3,S} = \widehat{m}_{t_S}^S + \widehat{\Psi}_{t_S}^S \widehat{m}_{t_{S-1}}^S + \widehat{\Psi}_{t_S}^S \widehat{\Psi}_{t_{S-1}}^S \widehat{m}_{t_{S-2}}^S + \dots + \widehat{\Psi}_{t_S}^S \dots \widehat{\Psi}_{t_{S^*+1}}^S \widehat{m}_{t_{S^*}}^{3,S}. \quad (14)$$

This shows that

$$\widehat{m}^{3,S} - \widehat{m}^{2,S} = \widehat{\Psi}_{t_S}^S \dots \widehat{\Psi}_{t_{S^*+1}}^S (\widehat{m}_{t_{S^*}}^{3,S} - \widehat{m}_{t_{S^*}}^S).$$

This equation can be used to prove the following result:

Lemma B.5. *If C_{A3} in Assumption (A3) is large enough it holds that with probability tending to one*

$$\|\widehat{m}^S - \widehat{m}^{3,S}\| \leq C\delta_{1,n}.$$

We now decompose $\widehat{m}^{3,S}$ into a stochastic and a bias term

$$\widehat{m}^{3,S} - m^0 = \widehat{m}^{A,S} + \widehat{m}^{B,S} - m^0,$$

where $\widehat{m}^{A,S} = \sum_{t \in T_r} \widehat{m}_t^{A,S}$ minimizes

$$\sum_{i=1}^n \left(\varepsilon_i - \sum_{t \in T_r} m_t(X_{i,t}) \right)^2$$

over all function $m_t : (0, 1]^{|t|} \rightarrow \mathbb{R}$ that are piecewise constant on the rectangles $\mathcal{I}_{t,l}^S : l = 1, \dots, L_{t,S}$ and $\widehat{m}^{B,S} = \sum_{t \in T_r} \widehat{m}_t^{B,S}$ minimizes

$$\sum_{i=1}^n \left(m^0(X_i) - \sum_{t \in T_r} m_t(X_{i,t}) \right)^2$$

over the same class of piecewise constant functions. We see that $\widehat{m}^{A,S}$ is the projection of ε onto an $(S+1)$ -dimensional linear subspace of \mathbb{R}^n . We conclude that

$$E \left[\frac{1}{n} \sum_{i=1}^n \left| \sum_{t \in T_r} \widehat{m}_t^{A,S}(X_{i,t}) \right|^2 \right] \leq (S+1)n^{-1}\sigma^2. \quad (15)$$

For the study of the bias term define $\bar{m}(x) = \sum_{t \in T_r} \bar{m}_t(x_t)$ with

$$\bar{m}_t(x_t) = \frac{1}{n|\mathcal{I}_{t,l}^S|} \sum_{i: X_{i,t} \in \mathcal{I}_{t,l}^S} m_t^0(X_{i,t})$$

for $x_t \in \mathcal{I}_{t,l}^S$. Now, by definition of $\widehat{m}^{B,S}$, we have that

$$\frac{1}{n} \sum_{i=1}^n \left| \sum_{t \in T_r} \widehat{m}_t^{B,S}(X_{i,t}) - m^0(X_i) \right|^2 \leq \frac{1}{n} \sum_{i=1}^n |\bar{m}(X_i) - m^0(X_i)|^2.$$

Furthermore, we have by an application of Assumption (A4) that

$$\frac{1}{n} \sum_{i=1}^n |\bar{m}(X_i) - m^0(X_i)|^2 \leq C \frac{1}{n} \sum_{i=1}^n \sum_{t \in T_r} \sum_{k \in t} \left(b_{t,k,l_t(X_{i,t})}^S - a_{t,k,l_t(X_{i,t})}^S \right)^2 \leq C \delta_{1,n}^2.$$

Using the same arguments as in the proof of Lemma B.2 one gets the same bound with empirical norm replaced by the $L_2(P)$ -norm $\|\cdot\|$. This concludes the proof of the theorem.

Proof of Theorem 5.2 We now introduce the super index v again which denotes the number of the respective tree family. Note that the bound of Lemma B.5 holds uniformly over $1 \leq v \leq V$. We can decompose $\hat{m}^{3,S,v}$ into a stochastic and a bias term

$$\hat{m}^{3,S,v} - m^0 = \hat{m}^{A,S,v} + \hat{m}^{B,S,v} - m^0$$

and we get from (15) that

$$E \left[\frac{1}{n} \sum_{i=1}^n \left| \sum_{t \in T_r} \frac{1}{V} \sum_{v=1}^V \hat{m}_t^{A,S,v}(X_{i,t}) \right|^2 \right] \leq (S+1)n^{-1}\sigma^2.$$

For the treatment of the averaged bias term note that for $t \in T_r$

$$\hat{m}_t^{B,S,v}(x_t) = \hat{m}_t^{B,S,v}(x_t) - \sum_{t' \neq t} \int \frac{\hat{p}_{t \cup t'}^{S,v}(x_{t \cup t'})}{\hat{p}_t^{S,v}(x_t)} \hat{m}_{t'}^{B,S,v}(x_{t'}) dx_{t' \setminus t}$$

where $\hat{m}_t^{B,S,v}(x_t) = \frac{1}{n|T_{t,l}^{S,v}|_n} \sum_{i: X_{i,t} \in T_{t,l}^{S,v}} m^0(X_i)$ for $x_t \in \mathcal{I}_{t,l}^{S,v}$. Now by subtracting $m_t^0(x_t)$ we get

$$\begin{aligned} \hat{m}_t^{B,S,v}(x_t) - m_t^0(x_t) &= \hat{m}_t^{B,S,v}(x_t) - \bar{m}_t^0(x_t) \\ &\quad - \sum_{t' \neq t} \int \left(\frac{\hat{p}_{t \cup t'}^{S,v}(x_{t \cup t'})}{\hat{p}_t^{S,v}(x_t)} \hat{m}_{t'}^{B,S,v}(x_{t'}) - \frac{p_{t \cup t'}(x_{t \cup t'})}{p_t(x_t)} m_{t'}^0(x_{t'}) \right) dx_{t' \setminus t} \end{aligned}$$

where $\bar{m}_t^0(x_t) = \int \frac{p(x)}{p_t(x_t)} m^0(x) dx_{\{1, \dots, d\} \setminus t}$. This can be rewritten as

$$\begin{aligned} \hat{m}_t^{B,S,v}(x_t) - m_t^0(x_t) &= \hat{m}_t^{B,S,v}(x_t) - \bar{m}_t^0(x_t) + \Delta_{1,t}^v(x_t) \\ &\quad - \sum_{t' \neq t} \int \frac{p_{t \cup t'}(x_{t \cup t'})}{p_t(x_t)} \left(\hat{m}_{t'}^{B,S,v}(x_{t'}) - m_{t'}^0(x_{t'}) \right) dx_{t' \setminus t} + \Delta_{2,t}^v(x_t), \end{aligned}$$

where

$$\begin{aligned} \Delta_{1,t}^v(x_t) &= - \left(\hat{p}_t^{S,v}(x_t) - p_t(x_t) \right) \sum_{t' \neq t} \int \frac{p_{t \cup t'}(x_{t \cup t'})}{p_t^2(x_t)} m_{t'}^0(x_{t'}) dx_{t' \setminus t} \\ &\quad - \sum_{t' \neq t} \int \frac{\hat{p}_{t \cup t'}^{S,v}(x_{t \cup t'}) - p_{t \cup t'}(x_{t \cup t'})}{p_t(x_t)} m_{t'}^0(x_{t'}) dx_{t' \setminus t}, \\ \Delta_{2,t}^v(x_t) &= \sum_{t' \neq t} \int \left(\frac{\hat{p}_{t \cup t'}^{S,v}(x_{t \cup t'})}{\hat{p}_t^{S,v}(x_t)} - \frac{p_{t \cup t'}(x_{t \cup t'})}{p_t(x_t)} \right) \left(\hat{m}_{t'}^{B,S,v}(x_{t'}) - m_{t'}^0(x_{t'}) \right) dx_{t' \setminus t} \\ &\quad - \frac{\left(\hat{p}_t^{S,v}(x_t) - p_t(x_t) \right)^2}{p_t^2(x_t) \hat{p}_t^{S,v}(x_t)} \sum_{t' \neq t} \int \hat{p}_{t \cup t'}^{S,v}(x_{t \cup t'}) \hat{m}_{t'}^{B,S,v}(x_{t'}) dx_{t' \setminus t} \\ &\quad + \frac{\left(\hat{p}_t^{S,v}(x_t) - p_t(x_t) \right)}{p_t^2(x_t)} \sum_{t' \neq t} \int p_{t \cup t'}(x_{t \cup t'}) (\hat{m}_{t'}^{B,S,v}(x_{t'}) - m_{t'}^0(x_{t'})) dx_{t' \setminus t}. \end{aligned}$$

By averaging the integral equations over v we get

$$\begin{aligned} \hat{m}_t^{B,S,+}(x_t) - m_t^0(x_t) &= \hat{m}_t^{B,S,+}(x_t) - \bar{m}_t^0(x_t) + \Delta_{1,t}(x_t) \\ &\quad - \sum_{t' \neq t} \int \frac{p_{t \cup t'}(x_{t \cup t'})}{p_t(x_t)} \left(\hat{m}_{t'}^{B,S,+}(x_{t'}) - m_{t'}^0(x_{t'}) \right) dx_{t' \setminus t} + \Delta_{2,t}(x_t), \end{aligned} \tag{16}$$

where $m_t^{B,S,+} = V^{-1} \sum_{v=1}^V m_t^{B,S,v}$, $\hat{m}_t^{B,S,+} = V^{-1} \sum_{v=1}^V \hat{m}_t^{B,S,v}$, $\Delta_{1,t} = V^{-1} \sum_{v=1}^V \Delta_{1,t}^v$ and $\Delta_{2,t} = V^{-1} \sum_{v=1}^V \Delta_{2,t}^v$.

We now argue that with probability tending to one

$$\|\Delta_{1,t}\|_1 \leq C\delta_{4,n}, \quad (17)$$

$$\|\Delta_{2,t}\|_1 \leq C(\delta_{2,n}(\delta_{1,n} + S^{1/2}n^{-1/2}) + \delta_{3,n}^2), \quad (18)$$

$$\|\widehat{m}_t^{B,S,+} - \bar{m}_t^0\|_1 \leq C(\delta_{4,n} + \delta_{3,n}^2). \quad (19)$$

Note that with $\Delta_t = \Delta_{1,t} + \Delta_{2,t} + \widehat{m}_t^{B,S,+} - \bar{m}_t^0$ we can rewrite (16) as

$$\widehat{m}^{B,S,+} - m^0 = \Delta_t + \Psi_t(\widehat{m}^{B,S,+} - m^0). \quad (20)$$

Order the elements of T_r as t_1, \dots, t_{2^r} . Iterative application of (20) gives that

$$\widehat{m}^{B,S,+} - m^0 = \Delta_+ + \Psi_+(\widehat{m}^{B,S,+} - m^0), \quad (21)$$

where $\Delta_+ = \Delta_{t_1} + \Psi_{t_1}\Delta_{t_2} + \dots + \Psi_{t_1}\dots\Psi_{t_{2^r-1}}\Delta_{t_{2^r}}$ and $\Psi_+ = \Psi_{t_1}\dots\Psi_{t_{2^r}}$. Because Ψ_+ is a complete operator we get from (12) that $\|\Psi_+\mu\| \leq \gamma\|\mu\|$ for $\mu \in \mathcal{H}_{add}$ with $\gamma < 1$. Furthermore, one can easily verify that $\|\Psi_+\mu\| \leq C\|\mu\|_1$ for $\mu \in \mathcal{H}_{add}$ with some constant $C > 0$. With the help of (17)–(19) this shows that $\|\Delta_+\|_1 \leq C\delta_n$ and $\|\Psi_+\Delta_+\| \leq C\delta_n$ with probability tending to one where $\delta_n = \delta_{2,n}(\delta_{1,n} + S^{1/2}n^{-1/2}) + \delta_{3,n}^2 + \delta_{4,n}$. From (21) we get that $\widehat{m}^{B,S,+} - m^0 = \Delta_+ + \Delta_{++}$ with $\Delta_{++} = \sum_{k=1}^{\infty} \Psi_+^k \Delta_+$. It holds with probability tending to one that $\|\Delta_{++}\| \leq C\delta_n$ which implies that $\|\Delta_{++}\|_1 \leq C\delta_n$. We conclude that $\|\widehat{m}^{B,S,+} - m^0\|_1 \leq C\delta_n$ with probability tending to one. This shows the statement of Theorem 5.2. It remains to verify (17)–(19). The first claim follows directly from Assumption (A7). For the proof of (18) one makes use of the bounds for $\widehat{m}_{t'}^{B,S,v} - m_{t'}^0$, $\widehat{p}_{t \cup t'}^{S,v} - p_{t \cup t'}$ and $\widehat{p}_t^{S,v} - p_t$ which we have shown during the proof of Theorem 5.1 and which

carry over to the averaged values. For the proof of (19) note that

$$\widehat{m}_t^{B,S,+}(x_t) - \bar{m}_t^0(x_t) = \Delta_{3,t}(x_t) + \Delta_{4,t}(x_t)$$

with

$$\begin{aligned} \Delta_{3,t}(x_t) &= \frac{\widehat{p}_t^{S,+}(x_t) - p_t(x_t)}{p_t(x_t)} \sum_{t' \neq t} \int p_{t \cup t'}(x_{t \cup t'}) m_{t'}^0(x_{t'}) dx_{t' \setminus t} \\ &\quad + \sum_{t' \neq t} \int \frac{\widehat{p}_{t \cup t'}^{S,+}(x_{t \cup t'}) - p_{t \cup t'}(x_{t \cup t'})}{p_t(x_t)} m_{t'}^0(x_{t'}) dx_{t' \setminus t}, \\ \Delta_{4,t}(x_t) &= -V^{-1} \sum_{v=1}^V \left(\widehat{p}_t^{S,v}(x_t) - p_t(x_t) \right) \\ &\quad \times \sum_{t' \neq t} \int \frac{\widehat{p}_{t \cup t'}^{S,v}(x_{t \cup t'}) - p_{t \cup t'}(x_{t \cup t'})}{p_t^2(x_t)} m_{t'}^0(x_{t'}) dx_{t' \setminus t} \\ &\quad + V^{-1} \sum_{v=1}^V \frac{\left(\widehat{p}_t^{S,v}(x_t) - p_t(x_t) \right)^2}{p_t^2(x_t) \widehat{p}_t^{S,v}(x_t)} \sum_{t' \neq t} \int \widehat{p}_{t \cup t'}^{S,v}(x_{t \cup t'}) m_{t'}^0(x_{t'}) dx_{t' \setminus t}. \end{aligned}$$

Using similar arguments as above, one can easily verify that $\|\Delta_{3,t}\|_{t,*} \leq C\delta_{4,n}$ and $\|\Delta_{4,t}\| \leq C\delta_{3,n}^2$, with probability tending to one. This concludes the proof of the theorem.

C Further Simulation Results

In this section, we provide further results from our simulation study omitted in the main part of this paper. The results are given in Tables 5–17 and further confirm the discussion of Section 5.

Table 5: For each method, we ran 40 simulations to find the optimal parameter combinations from the parameter range below, measured via sample mean squared error: $n^{-1} \sum_i (m(X_i) - \widehat{m}(X_i))^2$. The names of the parameters are drawn from their functional definitions in their respective R-packages.

Method	Parameter range
xgboost	<code>max.depth</code> = 1 (if additive), = 2,3,4 (if <code>interaction(2+)</code>), <code>eta</code> = 0.005, 0.01, 0.02, 0.04, 0.08, 0.16, 0.32, <code>nrounds</code> = 100, 300, 600, 1000, 3000, 5000, 7000.
ebm	<code>max_tree_splits</code> = 1, <code>learning_rate</code> = 0.005, 0.01, 0.02, 0.04, 0.08, 0.16, 0.32, <code>nrounds</code> = 100, 300, 600, 1000, 3000, 5000, 7000.
rpf	<code>max_interaction</code> = 1 (if additive), = 2 (if <code>interaction(2)</code>), = ∞ if (<code>interaction(∞)</code>), <code>t_try</code> = 0.25, 0.5, 0.75, <code>nsplits</code> = 10, 15, 20, 25, 30, 40, 50, 60, 80, 100, 120, 200 , <code>split_try</code> = 2, 5, 10, 20.
rf	<code>m_try</code> = $\lfloor d/4 \rfloor$, $\lfloor d/2 \rfloor$, $\lfloor 3d/4 \rfloor$, $\lfloor 7d/8 \rfloor$, $\lfloor d \rfloor$, <code>min.node.size</code> = 5, <code>ntrees</code> = 500, <code>replace</code> = TRUE,FALSE,
sbf	<code>bandwidth</code> = 0.1, 0.2, 0.3.
gam	<code>select</code> =TRUE, <code>method</code> = 'REM' (in sparse models), default settings (in dense models).
BART	<code>power(β)</code> = 1, 2, 3, <code>ntree</code> = 50,100,150,200,250,300, sparsity parameter = 0.6,0.75,0.9.
MARS	<code>degree</code> = 1, 2, 3, 4, 5, 6, 7, 8, 9, 10, <code>penalty</code> = 1, 2, 3, 4, 5, 6, 7, 8, 9, 10.

Table 6: Model 4: Additive Sparse Jump Model. We report the average MSE from 100 simulations. The standard deviations are provided in brackets.

Method	dim=4	dim=10	dim=30
xgboost (depth=1)	0.19 (0.029)	0.282 (0.044)	0.401 (0.045)
xgboost	0.198 (0.031)	0.265 (0.053)	0.286 (0.034)
xgboost-CV	0.209 (0.028)	0.281 (0.052)	0.313 (0.058)
rpf (max_interaction=1)	0.159 (0.033)	0.198 (0.075)	0.179 (0.041)
rpf (max_interaction=2)	0.185 (0.028)	0.24 (0.066)	0.259 (0.043)
rpf	0.192 (0.026)	0.251 (0.065)	0.282 (0.043)
rpf-CV	0.169 (0.033)	0.207 (0.072)	0.183 (0.042)
rf	0.274 (0.035)	0.322 (0.05)	0.375 (0.037)
sbfb	0.342 (0.049)	0.603 (0.053)	1.112 (0.138)
gam	0.41 (0.047)	0.406 (0.027)	0.431 (0.06)
BART	0.177 (0.047)	0.162 (0.038)	0.157 (0.034)
BART-CV	0.179 (0.051)	0.163 (0.041)	0.159 (0.036)
MARS	0.751 (0.136)	0.74 (0.104)	0.687 (0.123)
1-NN	2.393 (0.229)	3.029 (0.308)	3.512 (0.333)
average	1.276 (0.075)	1.25 (0.063)	1.213 (0.054)

Table 7: Model 7: Additive Dense Smooth Model. We report the average MSE from 100 simulations. The standard deviations are provided in brackets.

Method	dim=4	dim=10
xgboost (depth=1)	0.2 (0.035)	0.662 (0.059)
xgboost	0.273 (0.028)	1.233 (0.127)
xgboost-CV	0.209 (0.043)	0.673 (0.06)
rpf (max_interaction=1)	0.162 (0.025)	0.578 (0.068)
rpf (max_interaction=2)	0.191 (0.017)	0.798 (0.097)
rpf	0.222 (0.019)	1.052 (0.115)
rpf-CV	0.178 (0.03)	0.6 (0.072)
rf	0.567 (0.044)	10.527 (0.772)
sbfb	0.071 (0.021)	0.183 (0.026)
gam	0.055 (0.012)	0.171 (0.045)
BART	0.155 (0.023)	0.438 (0.053)
BART-CV	0.165 (0.032)	0.465 (0.094)
MARS	0.166 (0.035)	4.4 (0.36)
1-NN	2.05 (0.108)	11.634 (0.702)
average	7.71 (0.381)	18.986 (1.391)

Table 8: Model 8: Hierarchical-interaction Dense Smooth Model. We report the average MSE from 100 simulations. The standard deviations are provided in brackets.

Method	dim=4	dim=10
xgboost	0.645 (0.053)	2.895 (0.271)
xgboost-CV	0.678 (0.042)	3.013 (0.338)
rpf (max_interaction=2)	0.414 (0.047)	3.643 (0.349)
rpf	0.385 (0.034)	3.357 (0.372)
rpf-CV	0.413 (0.033)	3.665 (0.467)
rf	0.77 (0.034)	12.265 (1.447)
BART	0.34 (0.04)	1.889 (0.324)
BART-CV	0.354 (0.059)	2.133 (0.363)
MARS	0.624 (0.114)	10.885 (0.635)
1-NN	2.516 (0.141)	17.728 (1.215)
average	10.696 (0.621)	26.502 (1.892)

Table 9: Model 2: Hierarchical-interaction Sparse Smooth Model. We report the average MSE from 100 simulations. The standard deviations are provided in brackets.

Method	dim=4	dim=10	dim=30
xgboost (depth=2)	2.435 (0.157)	2.542 (0.15)	2.587 (0.152)
xgboost	0.374 (0.035)	0.481 (0.064)	0.557 (0.089)
xgboost-CV	0.393 (0.051)	0.499 (0.058)	0.563 (0.089)
rpf (max_interaction=1)	2.36 (0.165)	2.43 (0.17)	2.404 (0.145)
rpf (max_interaction=2)	0.248 (0.038)	0.327 (0.045)	0.408 (0.07)
rpf	0.263 (0.034)	0.357 (0.044)	0.452 (0.076)
rpf-CV	0.277 (0.039)	0.366 (0.051)	0.463 (0.083)
rf	0.432 (0.039)	0.575 (0.061)	0.671 (0.08)
sbfi	2.298 (0.168)	2.507 (0.181)	3.163 (0.207)
gam	2.242 (0.172)	2.311 (0.159)	2.277 (0.185)
BART	0.214 (0.03)	0.223 (0.04)	0.252 (0.037)
BART-CV	0.242 (0.043)	0.276 (0.053)	0.315 (0.047)
MARS	0.355 (0.089)	0.282 (0.038)	0.414 (0.126)
1-NN	2.068 (0.156)	5.988 (0.624)	11.059 (0.676)
average	8.366 (0.43)	8.086 (0.246)	8.207 (0.496)

Table 10: Model 3: Pure-interaction Sparse Smooth Model. We report the average MSE from 100 simulations. The standard deviations are provided in brackets.

Method	dim=4	dim=10	dim=30
xgboost (depth1)	2.176 (0.14)	2.236 (0.176)	2.183 (0.136)
xgboost	0.417 (0.082)	0.797 (0.16)	1.381 (0.234)
xgboost-CV	0.443 (0.078)	0.872 (0.136)	1.497 (0.326)
rpf (max_interaction=1)	2.172 (0.133)	2.236 (0.164)	2.199 (0.145)
rpf(max_interaction=2)	0.416 (0.082)	1.289 (0.224)	1.822 (0.208)
rpf	0.219 (0.035)	0.556 (0.143)	1.186 (0.236)
rpf-CV	0.233 (0.033)	0.603 (0.163)	1.313 (0.253)
rf	0.304 (0.047)	0.744 (0.305)	1.295 (0.317)
sbfi	2.249 (0.159)	2.473 (0.181)	3.133 (0.22)
gam	2.161 (0.13)	2.222 (0.172)	2.209 (0.168)
BART	0.168 (0.022)	0.172 (0.032)	0.202 (0.021)
BART-CV	0.192 (0.03)	0.199 (0.039)	0.223 (0.025)
MARS	0.245 (0.088)	0.831 (0.728)	0.429 (0.403)
1-NN	1.323 (0.117)	2.642 (0.317)	4.173 (0.413)
average	2.187 (0.125)	2.226 (0.174)	2.177 (0.146)

Table 11: Model 5: Hierarchical-interaction Sparse Jump Model. We report the average MSE from 100 simulations. The standard deviations are provided in brackets.

Method	dim=4	dim=10	dim=30
xgboost(depth=1)	2.974 (0.112)	3.046 (0.12)	3.098 (0.223)
xgboost	1.02 (0.152)	1.28 (0.16)	1.418 (0.156)
xgboost-CV	1.049 (0.125)	1.279 (0.157)	1.475 (0.185)
rpf (max_interaction=1)	2.941 (0.117)	2.942 (0.123)	2.913 (0.197)
rpf (max_interaction=2)	0.767 (0.096)	1.082 (0.139)	1.34 (0.132)
rpf	0.745 (0.089)	1.093 (0.142)	1.307 (0.113)
rpf-CV	0.769 (0.101)	1.167 (0.152)	1.404 (0.14)
rf	0.914 (0.091)	1.237 (0.121)	1.415 (0.152)
sbfi	2.791 (0.098)	2.926 (0.12)	3.756 (0.284)
gam	2.782 (0.085)	2.728 (0.105)	2.793 (0.208)
BART	0.611 (0.078)	0.644 (0.106)	0.67 (0.094)
BART-CV	0.661 (0.111)	0.772 (0.173)	0.791 (0.133)
MARS	2.306 (0.17)	2.325 (0.145)	3.374 (2.716)
1-NN	4.559 (0.409)	8.883 (0.692)	13.434 (0.674)
average	8.721 (0.334)	8.449 (0.229)	8.638 (0.412)

Table 12: Model 6: Pure-interaction Sparse Jump Model. We report the average MSE from 100 simulations. The standard deviations are provided in brackets.

Method	dim=4	dim=10	dim=30	
xgboost (depth=1)	2.662 (0.078)	2.616 (0.105)	2.565 (0.153)	
xgboost	-	1.034 (0.177)	1.723 (0.178)	2.337 (0.378)
xgboost-CV	-	1.196 (0.371)	2.056 (0.3)	2.481 (0.385)
rpf (max_interaction=1)	2.682 (0.076)	2.653 (0.103)	2.601 (0.155)	
rpf (max_interaction=2)	1.252 (0.164)	2.268 (0.13)	2.534 (0.175)	
rpf	0.834 (0.121)	1.729 (0.156)	2.337 (0.284)	
rpf-CV	0.886 (0.142)	1.939 (0.2)	2.438 (0.246)	
rf	0.805 (0.172)	1.696 (0.168)	2.276 (0.306)	
sbfi	2.757 (0.094)	2.893 (0.128)	3.705 (0.282)	
gam	2.645 (0.096)	2.617 (0.095)	2.674 (0.165)	
BART	0.583 (0.074)	0.632 (0.124)	0.798 (0.29)	
BART-CV	0.608 (0.106)	0.73 (0.184)	1.16 (0.655)	
MARS	2.324 (0.14)	2.549 (0.296)	2.522 (0.291)	
1-NN	3.769 (0.323)	5.459 (0.419)	6.247 (0.434)	
average	2.637 (0.092)	2.59 (0.106)	2.55 (0.14)	

Table 13: Model 8: Hierarchical-interaction Dense Smooth Model. We report the average MSE from 100 simulations. The standard deviations are provided in brackets.

Method	dim=4	dim=10
xgboost (depth=1)	3.509 (0.266)	10.108 (0.425)
xgboost	0.645 (0.053)	2.895 (0.271)
xgboost-CV	0.678 (0.042)	3.013 (0.338)
rpf (max_interaction=1)	3.408 (0.237)	9.717 (0.378)
rpf (max_interaction=2)	0.414 (0.047)	3.643 (0.349)
rpf	0.385 (0.034)	3.357 (0.372)
rpf-CV	0.413 (0.033)	3.665 (0.467)
rf	0.77 (0.034)	12.265 (1.447)
sbfi	3.42 (0.208)	9.215 (0.419)
gam	3.258 (0.227)	9.212 (0.483)
BART	0.34 (0.04)	1.889 (0.324)
BART-CV	0.354 (0.059)	2.133 (0.363)
MARS	0.624 (0.114)	10.885 (0.635)
1-NN	2.516 (0.141)	17.728 (1.215)
average	10.696 (0.621)	26.502 (1.892)

Table 14: Model 9: Pure-interaction Dense Smooth Model. We report the average MSE from 100 simulations. The standard deviations are provided in brackets.

Method	dim=4	dim=10
xgboost (depth=1)	3.108 (0.197)	8.091 (0.359)
xgboost	0.596 (0.063)	3.888 (0.411)
xgboost-CV	0.684 (0.069)	3.974 (0.508)
rpf (max_interaction=1)	3.119 (0.209)	8.156 (0.366)
rpf (max_interaction=2)	0.712 (0.101)	5.944 (0.324)
rpf	0.38 (0.049)	4.747 (0.329)
rpf-CV	0.395 (0.055)	4.789 (0.335)
rf	0.657 (0.074)	5.784 (0.409)
sbf	3.385 (0.183)	9.177 (0.479)
gam	3.109 (0.216)	8.183 (0.389)
BART	0.266 (0.034)	1.425 (0.183)
BART-CV	0.299 (0.054)	1.738 (0.254)
MARS	0.618 (0.552)	6.257 (0.824)
1-NN	1.482 (0.126)	7.358 (0.514)
average	3.156 (0.221)	8.109 (0.363)

Table 15: Model 10: Additive Dense Jump Model. We report the average MSE from 100 simulations. The standard deviations are provided in brackets.

Method	dim=4	dim=10
xgboost (depth=1)	0.325 (0.068)	1.095 (0.106)
xgboost	0.376 (0.085)	1.437 (0.153)
xgboost-CV	0.36 (0.073)	1.187 (0.145)
rpf (max_interaction=1)	0.321 (0.047)	1.273 (0.161)
rpf (max_interaction=2)	0.402 (0.059)	2.18 (0.139)
rpf	0.429 (0.067)	2.804 (0.192)
rpf-CV	0.326 (0.051)	1.303 (0.166)
rf	0.807 (0.104)	4.051 (0.186)
sbf	0.588 (0.078)	1.685 (0.185)
gam	0.923 (0.15)	4.405 (0.379)
BART	0.369 (0.079)	1.164 (0.093)
BART-CV	0.39 (0.076)	1.436 (0.253)
MARS	1.749 (0.151)	5.424 (0.304)
1-NN	3.822 (0.296)	11.278 (1.097)
average	2.5 (0.116)	6.332 (0.41)

Table 16: Model 11: Hierarchical-interaction Dense Jump Model. We report the average MSE from 100 simulations. The standard deviations are provided in brackets.

Method	dim=4	dim=10
xgboost(depth=1)	4.19 (0.238)	13.112 (0.83)
xgboost	1.666 (0.159)	9.327 (0.594)
xgboost-CV	1.87 (0.312)	9.407 (0.653)
rpf(max_interaction=1)	4.19 (0.253)	12.997 (0.831)
rpf (max_interaction=2)	1.43 (0.205)	9.238 (0.648)
rpf	1.26 (0.165)	9 (0.64)
rpf-CV	1.303 (0.171)	9.441 (0.604)
rf	1.681 (0.14)	13.6 (1.247)
sbf	3.972 (0.254)	12.234 (0.688)
gam	3.997 (0.251)	12.524 (0.858)
BART	1.01 (0.121)	7.116 (0.653)
BART-CV	1.165 (0.224)	7.897 (0.917)
MARS	3.595 (0.15)	16.307 (1.266)
1-NN	5.839 (0.649)	30.736 (1.933)
average	11.471 (0.498)	29.623 (2.046)

Table 17: Model 12: Pure-interaction Dense Jump Model. We report the average MSE from 100 simulations. The standard deviations are provided in brackets.

Method	dim=4	dim=10
xgboost (depth=1)	3.787 (0.297)	11.106 (0.546)
xgboost	1.606 (0.164)	10.005 (0.531)
xgboost-CV	1.768 (0.456)	10.868 (0.648)
rpf (max_interaction=1)	3.816 (0.259)	11.246 (0.596)
rpf (max_interaction=2)	2.005 (0.237)	10.846 (0.488)
rpf	1.441 (0.187)	10.264 (0.433)
rpf-CV	1.564 (0.214)	10.582 (0.536)
rf	1.36 (0.175)	10.235 (0.424)
sbf	3.928 (0.262)	12.129 (0.639)
gam	3.794 (0.271)	11.154 (0.573)
BART	0.972 (0.129)	6.835 (0.579)
BART-CV	1.04 (0.158)	7.208 (0.775)
MARS	3.541 (0.289)	11.03 (0.574)
1-NN	4.819 (0.475)	19.802 (1.51)
average	3.768 (0.283)	11.03 (0.574)